AMERICAN SOCIETY FOR MICROBIOLOGY | Applied and Environmental Microbiology

Microbial Ecology | Full-Length Text

Genome-resolved adaptation strategies of *Rhodobacterales* to changing conditions in the Chesapeake and Delaware Bays

Mir Alvee Ahmed,[1] **Barbara J. Campbell**[1]

AUTHOR AFFILIATION See affiliation list on p. 18.

ABSTRACT The abundant and metabolically versatile aquatic bacterial order, *Rhodobacterales*, influences marine biogeochemical cycles. We assessed *Rhodobacterales* metagenome-assembled genome (MAG) abundance, estimated growth rates, and potential and expressed functions in the Chesapeake and Delaware Bays, two important US estuaries. Phylogenomics of draft and draft/closed *Rhodobacterales* genomes from this study and others placed 46 nearly complete MAGs from these bays into 11 genera, many were not well characterized. Their abundances varied between the bays and were influenced by temperature, salinity, and silicate and phosphate concentrations. *Rhodobacterales* genera possessed unique and shared genes for transporters, photoheterotrophy, complex carbon degradation, nitrogen, and sulfur metabolism reflecting their seasonal differences in abundance and activity. *Planktomarina* genomospecies were more ubiquitous than the more niche specialists, HIMB11, CPC320, LFER01, and MED-G52. Their estimated growth rates were correlated to various factors including phosphate and silicate concentrations, cell density, and light. Metatranscriptomic analysis of four abundant genomospecies commonly revealed that aerobic anoxygenic photoheterotrophy-associated transcripts were highly abundant at night. These *Rhodobacterales* also differentially expressed genes for CO oxidation and nutrient transport and use between different environmental conditions. Phosphate concentrations and light penetration in the Chesapeake Bay likely contributed to higher estimated growth rates of HIMB11 and LFER01, respectively, in summer where they maintained higher ribosome concentrations and prevented physiological gene expression constraints by downregulating transporter genes compared to the Delaware Bay. Our study highlights the spatial and temporal shifts in estuarine *Rhodobacterales* within and between these bays reflected through their abundance, unique metabolisms, estimated growth rates, and activity changes.

IMPORTANCE In the complex web of global biogeochemical nutrient cycling, the *Rhodobacterales* emerge as key players, exerting a profound influence through their abundance and dynamic activity. While previous studies have primarily investigated these organisms within marine ecosystems, this study delves into their roles within estuarine environments using a combination of metagenomic and metatranscriptomic analyses. We uncovered a range of *Rhodobacterales* genera, from generalists to specialists, each exhibiting distinct abundance patterns and gene expression profiles. This diversity equips them with the capacity to thrive amidst the varying environmental conditions encountered within dynamic estuarine habitats. Crucially, our findings illuminate the adaptable nature of estuarine *Rhodobacterales*, revealing their various energy production pathways and diverse resource management, especially during phytoplankton or algal blooms. Whether adopting a free-living or particle-attached existence, these organisms demonstrate remarkable flexibility in their metabolic strategies, underscoring their pivotal role in driving ecosystem dynamics within estuarine ecosystems.

Editor Jennifer F. Biddle, University of Delaware, Lewes, Delaware, USA

Address correspondence to Barbara J. Campbell, bcampb7@clemson.edu.

The authors declare no conflict of interest.

See the funding table on p. 18.

Received 25 November 2024
Accepted 27 November 2024
Published 8 January 2025

[This article was published on 8 January 2025 with an error in Acknowledgments. The error was corrected in the current version, posted on 7 February 2025.]

KEYWORDS *Rhodobacterales*, growth rate, metagenome-assembled genome, estuarine, genomospecies

The *Rhodobacterales* is one of the predominant and versatile orders found in both particle-attached (PA) and free-living (FL) fractions of aquatic environments, particularly in marine ecosystems. They also serve as important models for understanding marine microbial ecology (1–5). Previous studies, employing microscopy or culture-dependent approaches and 16S rRNA gene-based analyses, along with more recent 'omics studies, have highlighted the abundance and diverse metabolic activities of *Rhodobacterales* in marine waters and sediments (1, 6–8). However, limited research exists on the temporal and spatial taxonomic and functional variations of *Rhodobacterales* in estuarine environments (9).

The remarkable metabolic versatility of *Rhodobacterales* allows them to thrive in various marine ecosystems, including temperate and polar oceans, coastal areas, and deep sea environments (1). They may constitute a significant proportion of bacterial communities, accounting for up to 20% and 5%, respectively, of communities in coastal ecosystems and open ocean surface waters and are mostly associated with algal blooms (10). A well-studied clade within the *Rhodobacterales*, *Roseobacter*, uses different energy production and carbon acquisition mechanisms, including carbon monoxide, sulfur transformation abilities, hydrogen sulfide oxidation, and hydrocarbon degradation (8, 11–13). Some strains utilize bacteriochlorophyll *a* to capture light energy, while others rarely possess xanthorhodopsin or proteorhodopsin for light-driven processes (1).

The Chesapeake and Delaware Bays, located in the Mid-Atlantic region of the USA, offer excellent opportunities to study the diversity of microbes in different ecological niches. The Chesapeake Bay, the largest estuary of the United States (14, 15), exhibits strong salinity gradients where it receives substantial freshwater inflow, sediment deposition, and particles (16, 17). The bay is highly stratified, especially in summer (18). Factors such as temperature and substrate availability are key controls on bacterial abundance and production in the bay (16, 19). Phytoplankton production varies seasonally due to light availability and is influenced by nitrogen inputs from the Susquehanna River (20). On the other hand, the Delaware Bay receives 51% of total freshwater input from the Delaware River (17, 21). Unlike the Chesapeake Bay, the Delaware Bay is generally well mixed, and primary production is limited despite high nutrient concentrations because of high turbidity and reduced light penetration (22, 23). In the summer, urban inputs cause higher nitrogen and phosphorus concentrations in the Delaware in contrast to the Chesapeake Bay, where ammonium and phosphate concentrations typically increase through bottomwater regeneration. The Chesapeake has overall lower nitrate concentrations than the Delaware Bay, and the latter supports larger spring blooms as evidenced by chlorophyll *a* concentrations (24, 25).

Microbial communities in these bays vary with site-specific characteristics, and more importantly with seasonal variations, and their composition changes mostly with salinity and temperature (26, 27). Higher diversity indices in the upper Chesapeake Bay than in the lower Bay were identified in one prior study (28). *Alphaproteobacteria*, *Betaproteobacteria*, *Gammaproteobacteria*, *Cyanobacteria*, *Actinobacteria*, *Planctomycetes*, and *Bacteroidetes* were common in different seasons. Within the *Alphaproteobacteria*, SAR11 was particularly abundant in warm waters, whereas *Roseobacter* thrived in cold waters (19). In the Delaware Bay, microbial communities also changed along the salinity gradient. In the freshwaters of the estuary, *Actinobacteria*, *Verrucomicrobia,* and *Betaproteobacteria* dominated, while high salinity coastal waters contained high abundances of SAR11, and lower abundances of *Rhodobacterales*, *Gammaproteobacteria* and *Bacteroidetes* (27).

We propose that differences in salinity, freshwater input, turbidity and light penetration, nutrient availability, and physico-chemical parameters between the Chesapeake and Delaware Bays play a significant role in shaping *Rhodobacterales* composition, growth, and function in these estuaries. The greater stratification and longer retention

time in the Chesapeake compared to the Delaware estuary also may create conditions conducive to the development of a more estuary-specific microbial community. We explored how spatial and temporal environmental gradients shape the ecology of *Rhodobacterales* in estuarine systems and we found ubiquitous members like *Planktomarina*, and specialists like HIMB11, LFER01, or MED-G52 in samples from various salinity and seasons from two distinct bays.

RESULTS

Rhodobacterales metagenome-assembled genome

In total, 12 and 24 water samples were collected from the Chesapeake and Delaware Bays, respectively, for metagenome-assembled genome (MAG) construction. Delaware and Chesapeake Bay samples were collected during the spring, summer, and fall of 2014 or the spring and summer of 2015, respectively, from low (0.019–0.06 PSU), medium (15–22 PSU), and high (27–31 PSU) salinities (29, 30). For labeling, the first two letters of a sample name, like CPSpr15L08 or DESum29G08 indicated the bay (CP or DE for the Chesapeake and the Delaware Bay, respectively), followed by letters for the season of collection (Spr and Sum for Spring and Summer, respectively, and Fall), then numbers indicating salinity in PSU, and finally G08 or L08 to indicate larger (>0.8 µm) or smaller (<0.8 µm) size fractions. In addition, a D or N indicated samples collected during the day or at night, respectively. The MAG names were distinguished with an underscore after the metagenome label followed by associated bin numbers (e.g., DESpr20G08_bin_28).

From the 36 assembled metagenomes, 46 MAGs with >80% completeness and <5% contamination were taxonomically classified using GTDB-Tk as members of the order *Rhodobacterales* (31). The average size of the medium- to high-quality MAGs was 2.8 ± 0.53 Mbp and the average GC content was 52.6% ± 5.5% (Data Set S1). Both GTDB-Tk-based taxonomic affiliation and position in a phylogenomic tree indicated that these MAGs belonged to 11 *Rhodobacterales* genera, namely, *Amylibacter* (Am), *Boseongicola* (Bo), CPC320 (CP), HIMB11 (HI), LFER01 (LF), LGRT01 (LG), MED-G52 (ME), *Planktomarina* (Pl), *Roseicyclus* (Ro), *Sulfitobacter* (Su), and *Yoonia* (Yo) (Fig. 1) (31, 32). Abbreviated genus names were added to the representative MAG names for clarity. Each genus contained at least one MAG from this study with one or more *Rhodobacterales* genomes, MAGs, or single amplified genomes (SAGs) from other studies. Among the Chesapeake and Delaware Bay MAGs, 14 were related to *Planktomarina*, 6 to HIMB11 or *Yoonia*, 5 to *Sulfitobacter*, 4 to MED-G52, 3 to LFER01, 2 each were related to *Amylibacter*, CPC320 or *Roseicyclus*, and only one each was related to *Boseongicola* and LGRT01 (Fig. 1; Data Set S1). After dereplication at a 95% average nucleotide identity (ANI) cutoff to find representative genomospecies, *Sulfitobacter* and *Yoonia* each had three representative species; *Amylibacter*, MED-G52, and *Planktomarina* genera each had two, while *Boseongicola*, CPC320, HIMB11, LFER01, LGER01, and *Roseicyclus* each had one (Data Set S1).

In situ abundances

The *Rhodobacterales* MAGs assembled from the Chesapeake and Delaware Bay metagenomes represented between 0.1% and 12.2% or 0.4% and 24.3% of the entire community in samples as revealed by singleM or number of reads recruited per kilobase of MAG and gigabase of metagenome (RPKG) analyses, respectively (Fig. 2; Fig. S2) (36). Moreover, together these MAGs covered a significant portion (20.2%–4.8%) of all *Rhodobacterales* estimated through Kaiju read-based coverage analysis (Fig. S2) (37). Distinct patterns were observed in the RPKG profiles of the representative *Rhodobacterales* genomospecies, especially between salinities, seasons, and bays (Fig. 2). *Rhodobacterales* were not detected in low salinity samples but were abundant in all medium- and high-salinity samples. One *Planktomarina* genomospecies, Pl_DESpr20G08_bin_28, was especially abundant in both bays in spring and the Delaware Bay in summer while the other *Planktomarina* genomospecies, Pl_CPSpr30L08_38, was most abundant in high salinity

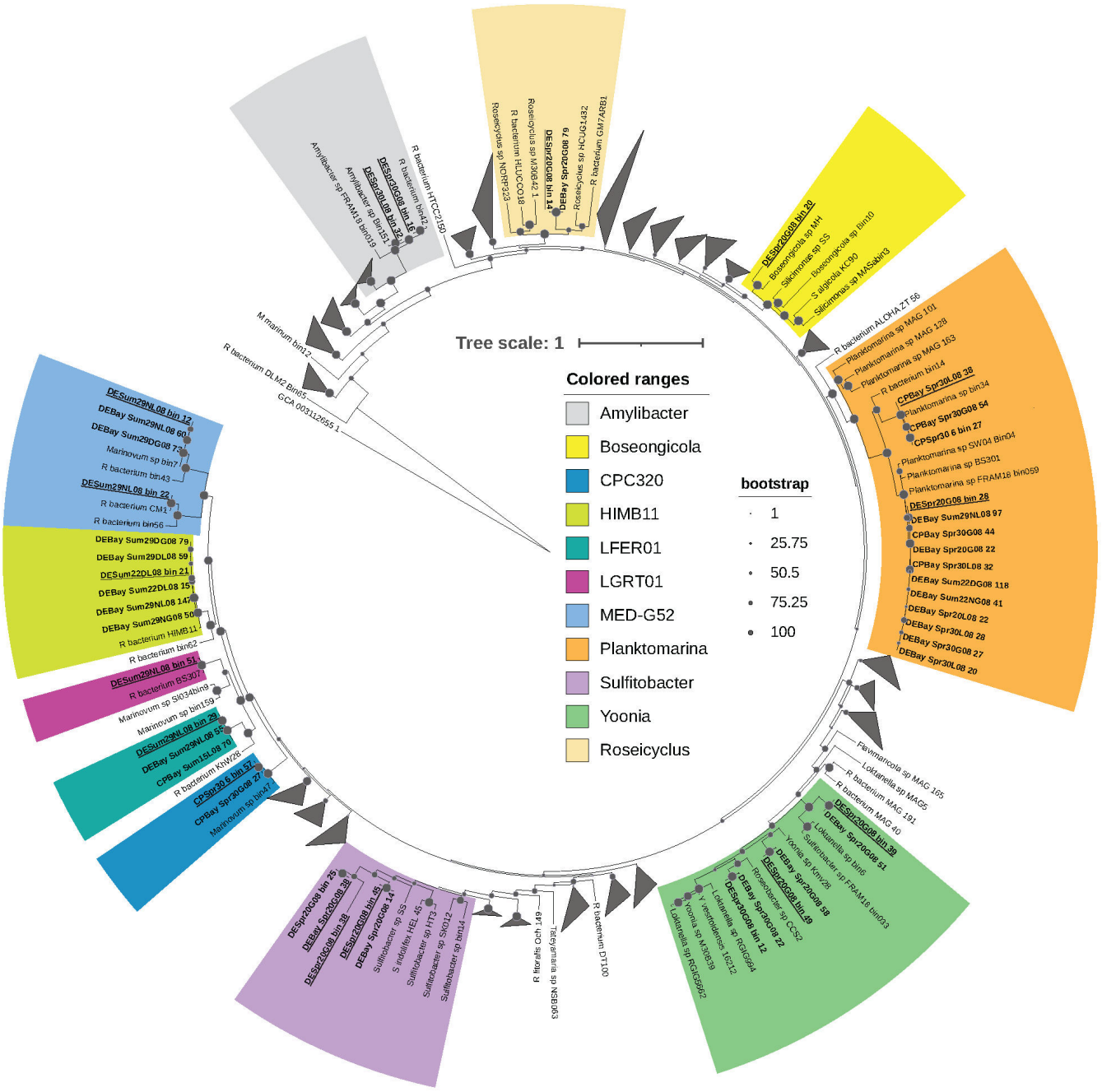

FIG 1 Phylogenomics of *Rhodobacterales* MAGs from the Delaware and Chesapeake Bays. A maximum likelihood tree of 28 concatenated single-copy ribosomal proteins derived using anvi'o from a total of 338 *Rhodobacterales* MAGs/genomes from this study and others (33, 34). The RAxML program was used to obtain the tree with the PROTGAMMALG model of rate heterogeneity (32). The tree was annotated in iTOL (35). Bootstrap values of 70% or higher from 1,000 sample trees were represented through dark circles on the nodes. A *Cyanobacteria* sp. was used to root the tree. Multiple genomes in clades without any MAG from this study were collapsed together into gray wedges. Bold text indicates MAGs from this study, and dereplicated ones are highlighted with underscores. Eleven genera to which MAGs from this study belonged were highlighted with colors. Abbreviations: CP = Chesapeake Bay; DE = Delaware Bay; Spr = Spring; Sum = Summer; the numbers following bay name and season indicate salinity in PSU; D = day; *N* = night; G08 = >0.8 µm, and L08 = <0.8 µm size fraction.

Chesapeake Bay spring samples, along with two *Sulfitobacter* genomospecies. All *Yoonia*, *Sulfitobacter,* and *Roseicyclus* genomospecies were abundant in Delaware Bay spring samples. *Boseongicola* genomospecies were abundant in medium-salinity and *Amylibacter* genomospecies were abundant in high-salinity Delaware Bay spring samples. HIMB11-, LFER01-, LGRT01-, and MED-G52-related genomospecies were abundant in

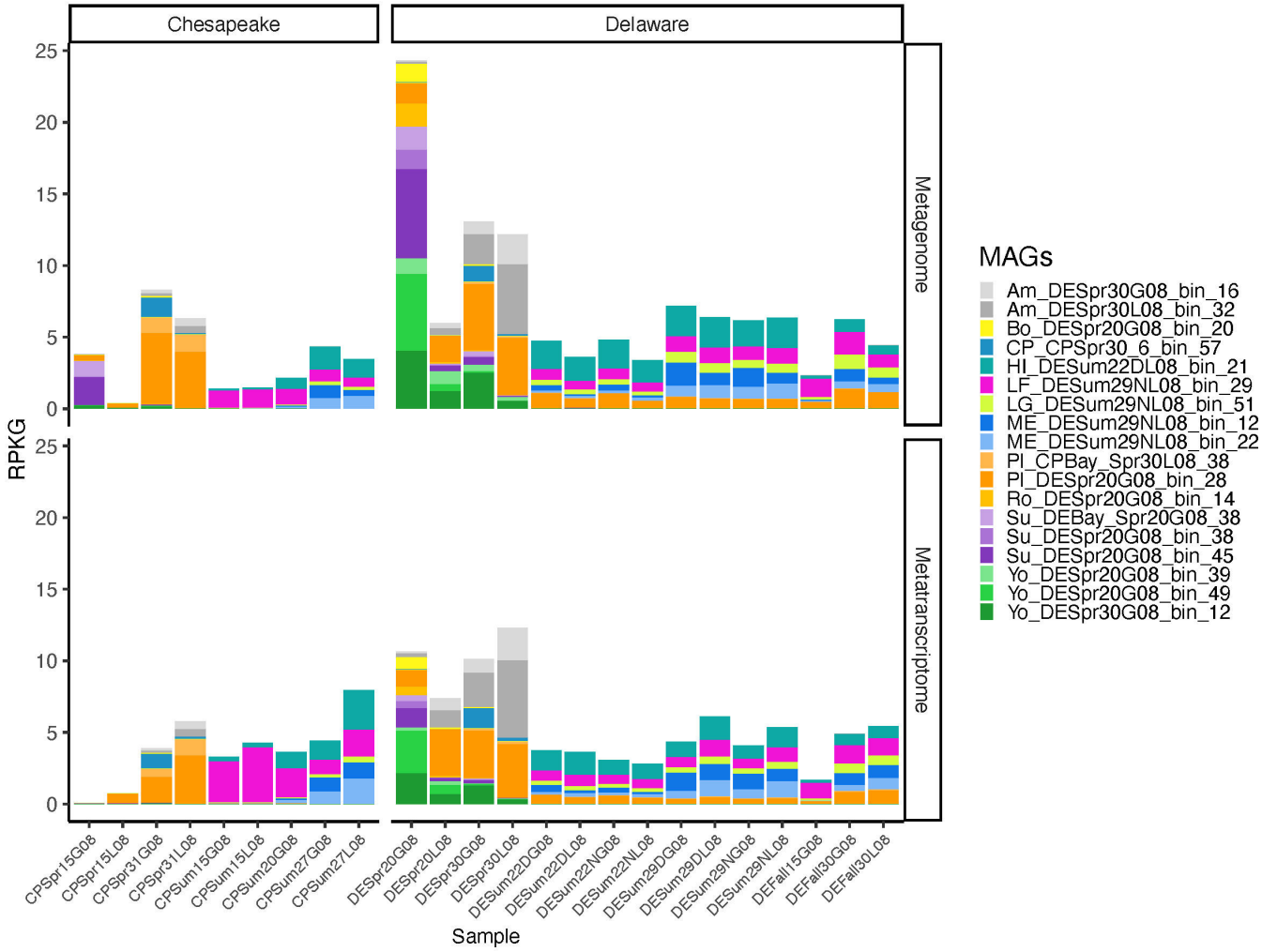

FIG 2 RPKG of *Rhodobacterales* in the Chesapeake and Delaware Bay metagenomes and metatranscriptomes. Abundance via RPKG values was calculated based on the featureCounts table and the total length of all ORFs in each representative MAG (38–40). Abbreviations: CP = Chesapeake Bay; DE = Delaware Bay; Spr = Spring; Sum = Summer; the numbers following indicate salinity in PSU; D = day; *N* = night; G08 = >0.8 µm, and L08 = <0.8 µm size fraction. Two letters at the beginning of a MAG indicate the genus to which it belongs according to GTDB-Tk taxonomy (31). Abbreviations: Am = *Amylibacter*; Bo = *Boseongicola*; CP = CPC320; HI = HIMB11; LF = LFER01; LG = LGRT01; ME = MED-G52; PI = *Planktomarina*; Ro = *Roseicyclus*; Su = *Sulfitobacter*; Yo = *Yoonia*.

summer from both bays. Most genomospecies were equally represented in the metagenomes and metatranscriptomes except the LFER01-related genomospecies, which had higher abundances in the metatranscriptomes than in metagenomes in the Chesapeake Bay summer samples.

Spearman correlation analysis between environmental variables and a Mantel test revealed that the average abundance, expressed as RPKG, of representative *Rhodobacterales* MAGs from these bays was significantly and positively correlated ($P < 0.05$) with salinity, temperature, and phosphate and silicate concentrations from summer samples (Fig. S3a) (41). However, a similar analysis was not done for spring due to the low number of samples. When analyzed individually, the abundance of *Planktomarina*, HIMB11, LFER01, and MED-G52 genomospecies was all positively correlated with temperature ($P < 0.05$) and silicate concentrations ($P < 0.1$), all but *Planktomarina* were positively correlated with phosphate concentrations ($P < 0.05$) and two (*Planktomarina* and MED-G52) were positively correlated with cell density ($P < 0.05$) (Fig. S3b and c).

Pangenome analyses

We performed pangenome analysis to determine the functional potentials of the 11 *Rhodobacterales* genera above, including all 46 MAGs recovered from the Chesapeake and Delaware Bay samples and 57 previously reported genomes/MAGs (31, 33, 42). Each of the 11 genera had more than 9 members on average, though CPC320 had only three and *Planktomarina* had 23 members (Data Set S2). Genes found in all genera featured full pathways for glycolysis (Embden-Meyerhof pathway), pentose phosphate, citrate (TCA or Krebs), and glyoxylate cycles. Moreover, several electron transport chain complexes (I–V), associated with aerobic respiration, were found to be fully covered in the pangenome. Among the common metabolic processes encoded by genes in most *Rhodobacterales* genera found in these bays were C1 metabolism, alcohol production, thiosulphate oxidation to sulfate through the sulfur oxidation (Sox) enzyme system, and the light reactions in photosynthesis (Fig. 3). Genes related to nitrogen-transforming processes—such as nitrogen fixation, nitrification, denitrification, and dissimilatory nitrate reduction to ammonium were not common in the pangenome.

Differences in metabolic pathways

Rhodobacterales genera differed in their metabolic potentials on many occasions. For instance, all members of CPC320, HIMB11, LFER01, MED-G52, and *Planktomarina* lacked genes associated with nitrogen-transforming processes. Among the spring dominant

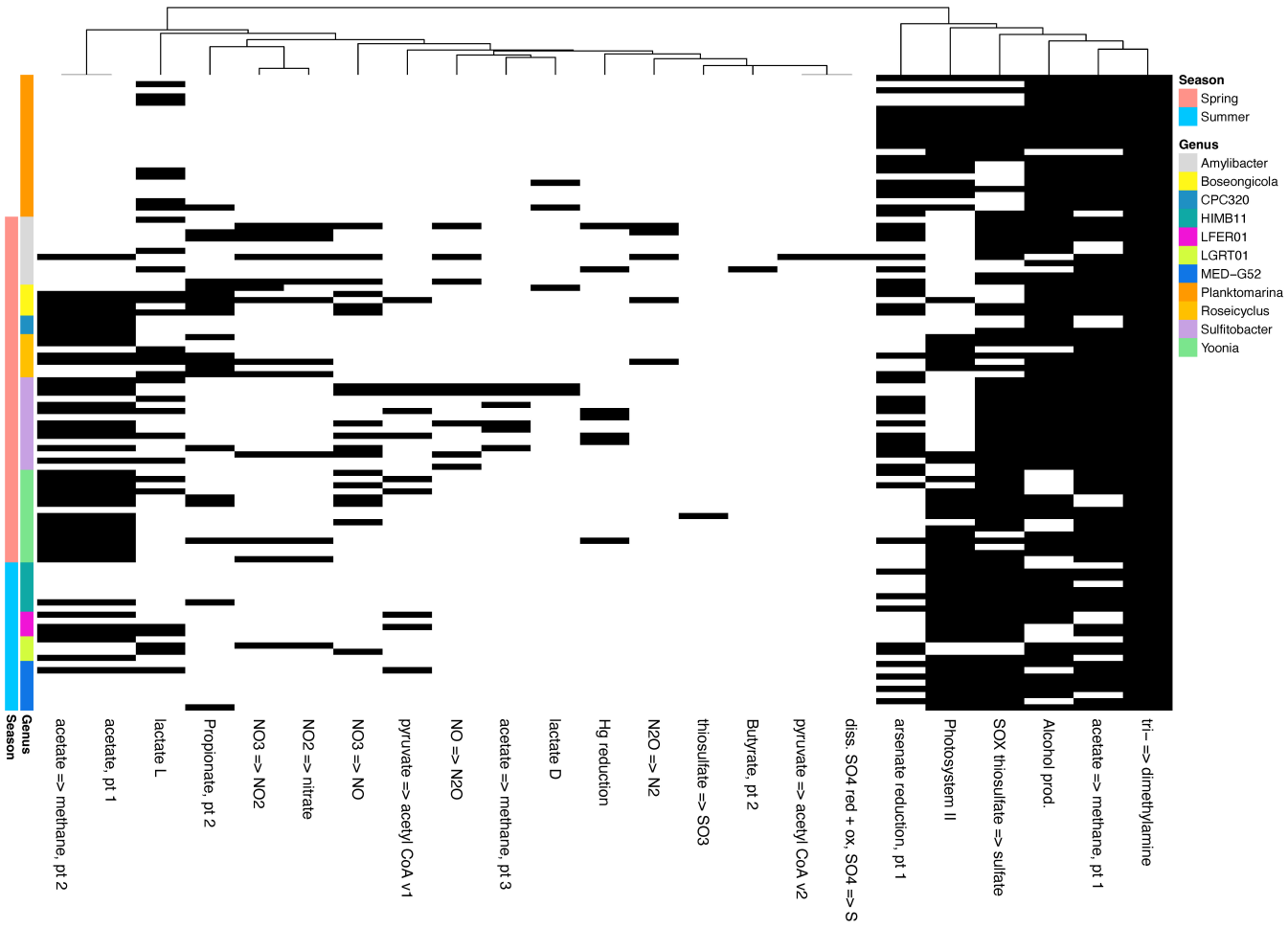

FIG 3 Pangenome analysis of 11 selected *Rhodobacterales* genera. In all members of 11 genera with representatives found in the Chesapeake and Delaware Bays, genes were annotated using DRAM (42), and the presence of key genes of select metabolic pathways is shown. The color bar on the left indicates the different genera and their seasonal dominance.

genera, *Amylibacter* uniquely possessed the ability to break butyrate, convert pyruvate to acetyl CoA, and transform sulfate to sulfide through the dissimilatory reduction process. Unlike the other genera, both *Amylibacter* and *Sulfitobacter* lacked genes for light reactions for aerobic anoxygenic phototrophy (AAP). *Sulfitobacter* were among the few with the potential to use polyphenolics. *Yoonia* uniquely had genes involved in the metabolism of xyloglucan and sulf-polysaccharides and the oxidation of thiosulfate to sulfite (Fig. 3; Data Set S2).

Transporters

Transporter genes were among the most abundant in all members of the pangenome. We identified 38 transporter genes that were present in >50% of members of each genus, and ~13% of such genes were found in all MAGs (Data Set S2). Such common genes included *livFH*, ABC.PE.P, and ABC.FE.SP for branched-chain amino acid, peptides/nickel transport, and iron transport systems, respectively. Some transporter genes were uniquely present or absent in a genus (Fig. S4). For instance, *glpPQV*, and *rhaPS* for glycerol, and rhamnose transport, respectively, were found in all members of CPC320. Genes for alpha-1,4-digalacturonate and putative thiamine transport systems were uniquely observed in >75% of members of *Roseicyclus* and *Yoonia*, respectively. Though common in nine genera, *Sulfitobacter* and *Yoonia* lacked the *mlaC* gene for phospholipid transport system.

CAZymes

The differential presence of carbohydrate-active enzymes (CAZymes) was assessed in the pangenome, as carbohydrates from various sources provide energy for estuarine microbes, especially for PA bacteria (43). The number of CAZy genes in representative *Rhodobacterales* MAGs ranged from 1 to 50 and they belonged to 53 CAZy subfamilies (Fig. S5) (44–46). *Sulfitobacter*, *Roseicyclus*, *Yoonia*, and *Planktomarina* MAGs contained a variety of CAZymes. However, representative MAGs of *Amylibacter*, HIMB11, LFER01, and MED-G52 were less versatile than others in regard to the types and numbers of CAZymes they contained. Sub-families AA3_2 (auxiliary activities), GH23 (glycoside hydrolases), GT2, GT4, GT19, and GT28 (glycosyl transferases) were present in about 80% of the analyzed genera. The number of GT2 and GT4 genes was much higher in the *Roseicyclus* and *Sulfitobacter* representative MAGs compared to the others.

In situ growth estimates

Analyzing the true growth rates of *Rhodobacterales* members in these two bays was beyond the scope of the study. However, peak-to-trough ratio (PTR)-based analyses (47) of representative *Rhodobacterales* genomospecies MAGs from our data set indicated differences in estimated growth rates, which varied among taxa (Table 1) and depended on environmental conditions. A significant positive correlation ($P < 0.05$) was found between PTRs of *Planktomarina*, HIMB11, LFER01 genomospecies, and various combinations of light availability, cell density, and phosphate concentrations (Fig. 4). *Planktomarina* and HIMB11 growth rate estimates were correlated with phosphate concentrations ($P < 0.05$), HIMB11 growth rate was also correlated with cell numbers ($P < 0.05$) and weakly with silicate ($P < 0.1$) while LFER01 growth rate was correlated with light (PAR and Secchi) and weakly with salinity.

Among all representative genomospecies, estimated growth rates in the spring were the highest in the *Amylibacter* MAG, ranging from 0.81 to 1.3 while those from CPC-320, *Sulfitobacter*, and *Yoonia*-related MAGs ranged from 0.33 to 0.85 (Table 1). For PI_DESpr20G08_bin_28, growth rates averaged 0.59 ± 0.12 in both bays in spring and less in Delaware Bay summer samples, averaging 0.45 ± 0.08. Growth rates from representative HIMB11, LFER01, and MED-G52 MAGs averaged 0.29–0.74 in summer. Overall, the summer genomospecies had higher average growth rates in the Chesapeake (0.55–0.69) compared to the Delaware Bay (0.44–0.58). Estimated growth rates in the

TABLE 1 Estimated growth rates of *Rhodobacterales* in the Chesapeake and Delaware Bays[a]

			Amylibacter		CPC320	HIMB11	LFER01	MED-G52		*Planktomarina*		*Sulfitobacter*		*Yoonia*
Bay	Season	PSU-SF	Am_16	Am_32	CP_57	HI_21	LF_ 29	ME_12	ME_22	Pl_38	Pl_28	Su_38	Su_45	Yo_12
CP	Spr	15G08									0.84	0.62	0.79	
		31G08		1.03	0.62					0.57	0.59			0.49
		31L08	1.29	0.89	0.56					0.64	0.65			
	Sum	15L08				0.54	0.58							
		20G08				0.64	0.53							
		27G08				0.73	0.49	0.68	0.55					
		27L08				0.69	0.60	0.63	0.65					
DE	Spr	20G08		0.81	0.51						0.52	0.55	0.50	0.69
		20L08	1.01	0.85							0.44		0.33	0.85
		30G08	1.00	0.84	0.63						0.56	0.52	0.52	0.68
		30L08	1.11	0.81	0.48					0.54	0.49			0.74
	Sum	22DG08				0.73	0.54	0.64	0.37		0.54			
		22DL08				0.49	0.39	0.46	0.36		0.36			
		22NG08				0.69	0.54	0.61	0.45		0.48			
		22NL08				0.69	0.52	0.63	0.40		0.42			
		29DG08				0.73	0.50	0.74	0.58		0.54			
		29DL08				0.55	0.47	0.64	0.49		0.36			
		29NG08				0.73	0.49	0.69	0.54		0.52			
		29NL08				0.55	0.43	0.64	0.47		0.37			
	Fall	15G08				0.52	0.36				0.37			
		15L08				0.56	0.41				0.40			
		30G08				0.55	0.30	0.62	0.49		0.48			
		30L08				0.49	0.29	0.56	0.39		0.32			

[a]PSU-SF: Salinity in PSU- Size fraction; CP = Chesapeake Bay; DE = Delaware Bay; Spr = Spring; Sum = Summer; D = day; N = night; abbreviated MAG names are mentioned in Data Set S2.

large size fraction were significantly higher (P < 0.05) than the small size fraction for Pl_DESpr20G08_bin_28 and HI_DESum22DL08_bin_21 and ranged from 0.37 to 0.59 and 0.51–0.73, respectively, in the large size fraction vs. 0.32–0.65 and 0.49–0.69, respectively, in the FL fraction. There were no significant differences in estimated growth rates

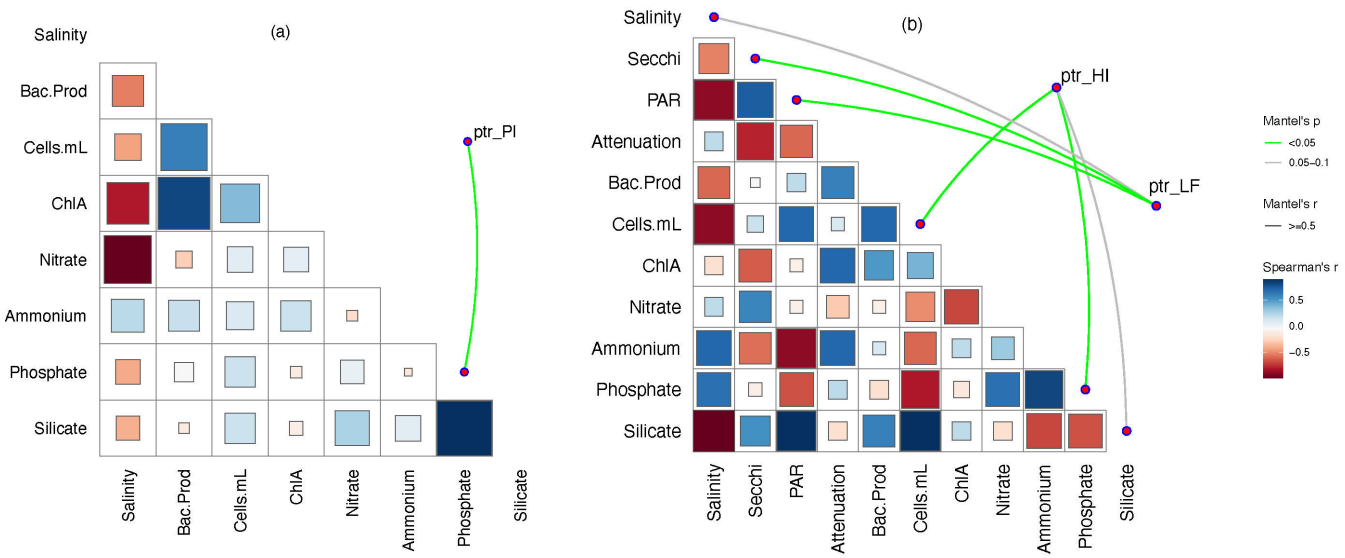

FIG 4 Relationships between estimated growth rates of *Rhodobacterales* and environmental factors. $\log_2$PTR values of genomospecies and related environmental parameters of samples were analyzed for Mantel's correlation and *P*-values using the vegan package in RStudio (47, 48). (a) *Planktomarina* (ptr_Pl) and (b) HIMB11 (ptr_HI) and LFER01 (ptr_LF).

between day and night for any of the MAGs. The codon usage bias-based program, gRodon (49), was also used to estimate the maximum growth rates of MAGs and indicated that two MED-G52 MAGs had the longest maximal doubling time of >9 h, whereas HIMB11- and *Sulfitobacter*-related MAGs had the shortest, with maximum doubling times of <2 h (Table 1; Data Set S1).

Rhodobacterales gene expression

We hypothesized that *Rhodobacterales* activities, as estimated by their gene expression, would reflect their relative abundance and estimated growth rates depending on environmental conditions. RNA-Seq data of four MAGs with relatively high abundance and estimated growth rates in multiple samples (HI_DESum22DL08_bin_21, ME_DESum29NL08_bin_12, PI_DESpr20G08_bin_28, and LF_DESum29NL08_bin_29) were analyzed from medium- and high-salinity metatranscriptome samples. The four genomospecies had distinct gene expression patterns that varied with environmental conditions, such as time of day, location (bay), season, and size fraction (Fig. 4). Significant differences in gene expression of all four genomospecies were observed between night and day samples. Other noticeable differences occurred between bays and seasons. Heatmaps of the top 50 highly expressed genes indicated common trends in activity between these MAGs (Fig. 5; Fig. S6). Transporters were the most highly expressed genes in all four MAGs. The largest differences in the number of differentially expressed genes between conditions was between bays, with an average of 8.6% and 7.6% of aggregated genes differentially expressed in the summer PA or FL size fraction, respectively, in three of the four MAGs (Table S1). Gene expression in the *Planktomarina*-related genomospecies was the least affected by all environmental

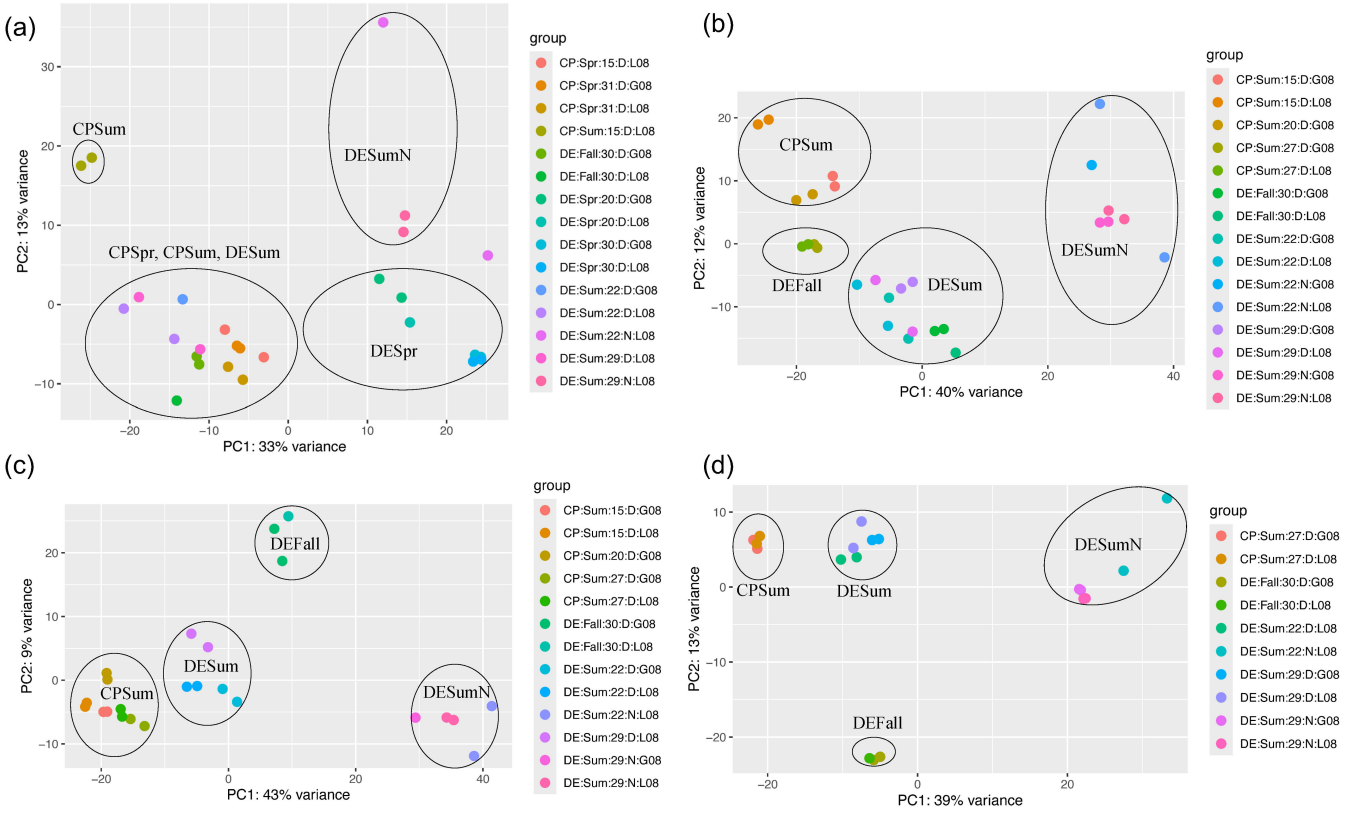

FIG 5 Ordination plots of gene transcripts from four abundant *Rhodobacterales* MAGs. PCA plot of DESeq2 normalized and transformed transcript abundances of representative MAGs from (a) *Planktomarina*, (b) HIMB11, (c) LFER01, and (d) MED-G52 in different samples, corresponding to different environmental conditions (50). Clusters were circled and labeled manually for visual comparison. Abbreviations: CP = Chesapeake Bay; DE = Delaware Bay; Spr = Spring; Sum = Summer; the numbers following bay name and season indicate salinity in PSU; D = day; *N* = night; G08 = >0.8 µm, and L08 = <0.8 µm size fraction.

conditions and the LFER01-related one was the most, with an average of 4.3% and 9.9% differentially expressed genes, respectively.

Gene expression differences between night and day

Daylight was the most common environmental factor influencing changes in gene expressions of the investigated *Rhodobacterales*. On average, 6.4% ± 2.7% of the total genes from these four MAGs were differentially expressed between night and day in both bays combined (Fig. 5; Table S1). All or a subset of genes from *pufABCLM* encoding reaction center proteins for AAP were expressed highly at night compared to the day in all four MAGs we tested in the Delaware Bay summer samples (Fig. 5; Fig. S6). In the HIMB11-related MAG, *bchXY* genes encoding bacteriochlorophyllide reductase subunits were also expressed more at night than during the day (Table S1). On the other hand, *coxLMS* genes encoding carbon monoxide dehydrogenase were expressed more in all four MAGs in the day compared to night samples. In addition, in the HIMB11-related MAG, genes encoding the tripartite tricarboxylate transporter family proteins TctA and TctB were expressed more during the day compared to night. Similar trends in transporter gene expression between night and day were seen in the other three MAGs.

Gene expression differences between the two bays

Rhodobacterales MAGs differed in the expression of certain genes between the two estuaries under the same conditions. In summer, the HIMB11 genomospecies had many genes like *tctAC*, *dctM*, *fadL*, *livHK,* and *yiaO* encoding transporter proteins of tripartite tricarboxylate, C4-decarboxylate, branched-chain amino acids, long-chain fatty acids, and TRAP-type transport system periplasmic proteins, respectively, significantly less expressed in the medium salinity FL size fraction samples of the Chesapeake compared to the Delaware Bay (Data Set S3). By contrast, expression of genes such as *rplBEMNQSUVX* and *rpsAGKLMNOQU*, responsible for encoding the large and small ribosomal subunits, respectively, were higher in the Chesapeake compared to Delaware under identical conditions. Furthermore, genes including *argF* and *acpP*, which encode anabolic enzymes for arginine and various secondary metabolite biosynthesis, respectively, showed higher expression levels in the Chesapeake than in the Delaware Bay. In the LFER01-related MAG, a trend of significantly higher expression of genes encoding ribosomal proteins (*rplBKMNOSUXY* and *rpsADGLMT*) in summer medium salinity FL samples from the Chesapeake compared to the Delaware Bay was observed. Moreover, expression of genes like *livK*, *tctC*, *yiaO*, and *proWX* encoding various transporters was lower in the Chesapeake than the Delaware Bay. In the MED-G52 genomospecies, only *rpsU* gene expression was significantly higher in high-salinity PA samples in the Chesapeake than in the Delaware Bay during summer. However, expression of genes like *tct*, *yia*, *liv,* and *pro* encoding various transporters was less in the Chesapeake than the Delaware Bay under the same conditions. For the *Planktomarina*-related genomospecies, differential ribosomal protein expression in the Chesapeake than the Delaware Bay was mostly insignificant except for the *rplM* gene which had higher expression in the former than the latter during spring. However, gene expression of transporters was significantly higher in the Delaware than in the Chesapeake Bay in the spring.

Other gene expression differences

Gene expression also varied with season, salinity, or size fraction (Data Set S3; Fig. 5 and Fig. 6; Fig. S6). For the HIMB11-related MAG, genes encoding tripartite-type tricarboxylate transporter TctC and (R)-benzylsuccinyl-CoA dehydrogenase were more highly expressed in summer compared to fall. In *Planktomarina*, transporter proteins were expressed more in spring than the fall (Data Set S3). In addition, *bchXY* genes and others involved in light harvesting were expressed in the *Planktomarina*-related MAG more in the fall compared to the summer. In spring, *alkB* for alpha-ketoglutarate-dependent dioxygenase and a pectate lyase superfamily gene and many genes for proteins of uncharacterized functions were expressed more compared to fall in this same MAG.

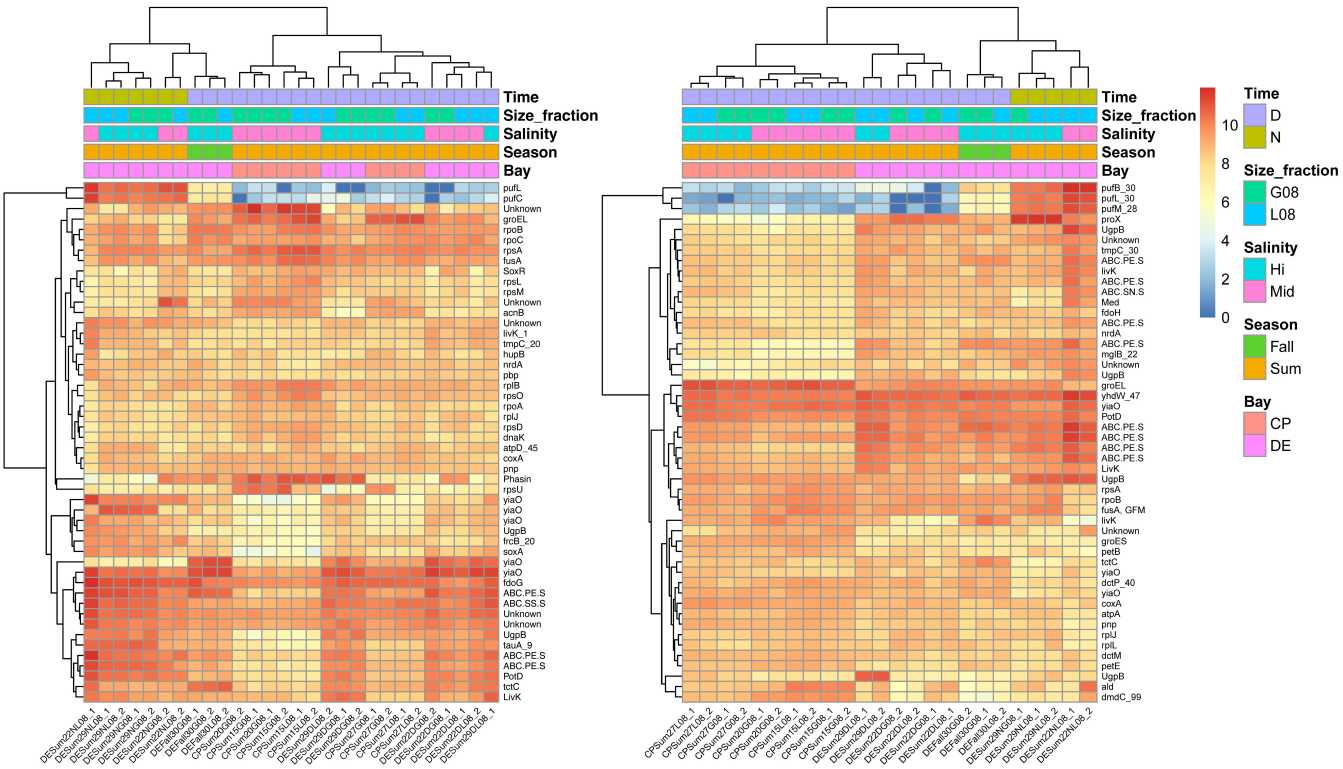

FIG 6 Top 50 most highly expressed genes of (left) HI_DESum22DL08_bin_21 and (right) LF_DESum29NL08_bin_29 in varying conditions. The most highly expressed 50 genes of these genomospecies were identified using DESeq2 (50). Abbreviations: CP = Chesapeake Bay; DE = Delaware Bay; Sum = Summer; # =salinity in PSU; G08 = >0.8 µm and L08 = <0.8 µm size fractions; # =RNA1 or RNA2; D = Day; *N* = Night. The gene symbol key is noted in the supplemental material.

Only a few genes were differentially expressed between salinities or bacterial size fractions (Table S1). In the *Planktomarina*-related MAG, genes encoding proteins for dimethylsulfoniopropionate (DMSP) degradation (DmdA), the phosphate transport protein (SphX), and L-cystate sulfo-lyase (CuvA) had higher expression in medium- compared to high-salinity spring samples in the Chesapeake Bay. On the other hand, genes such as *sugB* and *malK* for trehalose transport system permease and maltose/maltodextrin import ATP-binding protein, respectively, were more expressed in spring high salinities compared to medium salinities. In the HIMB11-related MAG, *rpmGH* and *rpsU* genes for the large and small ribosomal subunits, respectively, were expressed more in the PA compared to the FL size fraction in the Chesapeake Bay during summer. However, *rplCENQSU* and *rpsALO* for large and small ribosomal subunits, respectively, were expressed more in the small size fraction than the large fraction. The expression of genes encoding transporters was not significantly different between the two size fractions in the Chesapeake Bay.

DISCUSSION

The *Rhodobacterales* are a versatile aquatic bacterial order and can comprise up to a quarter of the total marine bacterioplankton (6, 10, 51). They are chemoheterotrophs and many can utilize light, sulfur, and CO for additional energy (6, 52). In the current study, we identified 18 *Rhodobacterales* genomospecies within 11 genera which varied in their metabolic and environmental niches as evidenced by genomic, abundance, estimated growth rate, and activity differences. In the Delaware Bay, *Rhodobacterales* relative abundance (as reflected by RPKG) in our study was up to 24% which was close to ~20% found previously (27). Many genomospecies inhabited the same environment, were relatively equal in their abundance, and had similar overall metabolisms. However, most

contained specific substrate-utilization and energy-production potentials and activities that varied with season, nutrient concentrations, or time of day.

Wide metabolic potentials of *Rhodobacterales* from the Delaware and Chesapeake Bays

Roseobacters have been considered "opportunitrophs" adapting to various lifestyles with their flexible genomes (53). As with other studies, most of the *Rhodobacterales* genomospecies found in this study could be considered specialists adapted better to a specific season and salinity as seen with other taxa (54, 55). However, a sharp delineation between generalist and specialist *Rhodobacterales* may be unclear, especially during blooms when both types are active (56, 57). In agreement with this, the *Rhodobacterales* in these bays exhibited a wide range of metabolic potentials, indicating their diverse roles in biogeochemical cycling, with many genes, especially transport-related ones, present in only a subset of the examined genera. However, the *Planktomarina* genomospecies Pl_DESpr20G08_bin_28 was seen in all seasons and both bays in mid and high salinities. Its estimated growth rate did not vary much, nor did the percentage of differentially expressed genes between various conditions. These combined observations support the notion that *Planktomarina* can potentially adopt a generalist lifestyle (55).

Multiple energy production mechanisms of *Rhodobacterales* in eutrophic ecosystems

Rhodobacterales contained several energy production mechanisms in these two eutrophic estuarine ecosystems. Nine out of eleven genera analyzed from these two bays contained genes necessary to use CO, folate, thiosulfate, and light for energy production, indicating their lithotrophic potential. To provide retention of organic carbon in marine food webs, the prevalence of *cox* genes in Roseobacters is almost universal and well documented from studies by Moran et al., Newton et al., and Cunliff et al. (13, 58, 59). Moreover, folate biosynthesis of *Dinoroseobacter shibae* was reported as an integral part of symbiosis with the alga *Ostreococcus tauri* underlining the importance of this metabolic ability (60). Roseobacters are well known for their ability to use sulfur and dimethyl sulfur compounds for energy production, especially after phytoplankton blooms, influencing the global sulfur cycle (2, 12, 61). Thiosulfate oxidase and sulfite dehydrogenase encoding genes found in most genomospecies were expressed more in high- compared to low- and mid-salinity samples in both bays, indicating the importance of sulfur-based lithotrophy in higher salinity waters. Similar to another study, the *dmdA* gene for the DMSP cleavage pathway was expressed by LFER01, HIMB11, and *Planktomarina* in both bays (62). Almost all *Rhodobacterales* from our study, except the genera *Amylibacter*, *Boseongicola,* and *Sulfitobacter,* would be considered AAP bacteria, as they contained and expressed genes for acquiring light energy through AAP. AAP genes were also commonly found in other Chesapeake and Delaware Bay studies (63, 64). Preheim et al. found many species contained *pufL* and *pufM*, and *Planktomarina* was the most common among them (63). While no significant differences in growth rates were observed between day and night, the nighttime expression of AAP genes may represent a preparatory strategy for diurnal energy harvesting (65, 66).

Relative abundance and estimated growth rates

A combination of estimated growth rates plus abundance provided a better understanding of environmental effects on the presence and activities of this taxonomic order than the latter alone, which agrees with other studies (27, 47, 67, 68). As there were no significant difference in growth rates between day and night, they probably do not maintain a circadian rhythm like Cyanobacteria (69). Their estimated growth rates may be related to genome size and lifestyle; small, FL, oligotrophic generalists are more apt to be slow growing than larger, PA copiotrophs with more specialized metabolic strategies

(70). Both HIMB11 and *Planktomarina* genomospecies had higher estimated growth rates in the PA compared to the FL fraction. This suggests their ability to use nutrients from particles or larger cells such as phytoplankton for biomass production.

Rhodobacterales abundance and estimated growth rates likely have some shared control mechanisms, as total and individual *Rhodobacterales* abundances and estimated replication rates correlated with phosphate and silicate concentrations from both bays. *Rhodobacterales* was found among the efficient dissolved organic phosphorus hydrolyzers using alkaline phosphatase in the Northwestern Mediterranean Sea (71, 72). Previous studies found silicate a key component supporting diatom blooms which likely provide organic carbon and nitrogen to various *Rhodobacterales* allowing for fast growth (56, 73). A *Rhodobacterales*, *Ruegeria pomeroyi* DSS-3, expressed more transporters to get various amino acids, nucleosides, and organic sulfur compounds from exometabolites in a microcosm with the diatom, *Thalassiosira pseudonana* (74). Previously, salinity was reported as the key factor in controlling marine bacterioplankton (27) and we also found it important for the average abundance of *Rhodobacterales*, especially *Planktomarina* and MED-G52. The RCA (*Roseobacter* clade affiliated) cluster abundance in the North Sea was found inversely correlated with salinity which ranged there from ~28 to 35 PSU, which we did not observe in our study covering freshwater to marine salinities. We did not find medium- or high-quality *Rhodobacterales* MAGs in low-salinity samples, possibly due to excessive species heterogeneity (51).

Environmental factors affecting *Rhodobacterales* estimated growth rates varied among the tested genomospecies. For example, estimated growth rates of both *Planktomarina* and HIMB11 were correlated with phosphate concentrations indicating their higher replication in phosphate-rich environments. The estimated growth rate of LFER01 was affected by PAR and Secchi disk depth (light availability) indicating that an increasing light promoted photoheterotrophy in this strain. Other environmental factors not measured here, such as carbon and sulfur concentrations and types, may also help explain differences in abundance vs. estimated growth rates.

Ubiquity and activity of *Planktomarina* in these estuaries

Planktomarina genomospecies were ubiquitous in both bays and in the spring, summer, and fall in Delaware bay, specifically with a higher abundance of the *Planktomarina*-related MAG PI_DESpr20G08_bin_28 in spring compared to summer. In Delaware Bay, *Planktomarina* estimated growth rates and transcript abundances were higher in spring than fall and may be related to daylight differences during the sampling time of 07:00 hours. These might indicate the efficiency of this genomospecies in using available resources in different seasons and locations. Previously, *Planktomarina* were reported to thrive in various marine ecosystems, successfully interacting with flora and fauna and producing energy using AAP, sulfur, and CO metabolisms (55, 75). Here, a *Planktomarina*-related MAG from the spring had higher growth rates in the PA than the FL fractions, and this agreed with other studies where some PA bacteria were found to be more active than many FL bacteria in estuaries (27). However, *Planktomarina* MAGs and amplicon sequence variants (ASVs) were less abundant in PA fraction than the FL fraction in samples collected from the southern North Sea and the Southern Ocean, respectively (76, 77). Our results also indicate differences in gene expression of important PA-associated functions in *Planktomarina*. In Delaware Bay, highly expressed genes during summer were in the ABC-type xylose transport system, followed by TRAP transporters and these gene products might help in acquiring bloom-associated metabolites. Moreover, high expression of the *livK* gene for the transport of branched-chain amino acid there suggests their competitive advantage when attached to larger particles to get low-molecular-weight substrates (78). Also, higher expression of the pectate lyase gene in spring compared to fall suggested more need for this enzyme to degrade pectin, a major cell wall component of eukaryotic phytoplankton and to help colonize particles containing mixed polysaccharide pools (79). The *Planktomarina*-related MAG expressed more ABC-type transporters likely acting as osmoprotectants (80) in

high- compared to medium-salinity samples. In addition, phosphate transporters and AAP genes were expressed significantly more in medium than high salinity, and sugar transporters and DMSP demethylase were expressed more in high compared to medium salinities. These protein products likely help the adaptation of *Planktomarina* to rapidly changing estuarine environments.

Rhodobacterales abundance and activity in the spring

The abundance and estimated growth rate patterns of *Rhodobacterales* were distinct in both bays, depending on the season. In spring, *Amylibacter*, *Sulfitobacter,* and *Yoonia* were highly abundant and had relatively high estimated rates of replication, especially in Delaware Bay. Overall, these spring genera had similar metabolic potentials, especially regarding sulfur, nitrogen, and C1 metabolism. In addition, they had higher numbers and diversities of CAZymes than other genera which enable them to use bloom-derived carbohydrates. These *Rhodobacterales* possessed genes for phosphate and sulfate transporters, likely enabling them to use eukaryotic bloom-derived organic phosphates and sulfates (81). Also, their activity was likely controlled by eukaryotic phytoplankton blooms prevalent during that season, as evidenced by the highest level of chlorophyll *a* in the mid-salinity Delaware Bay spring sample compared to other samples as well as with historically measured phytoplankton blooms in the spring (29, 82). Previously, FL *Amylibacter* was found associated with spring phytoplankton blooms and after the first bloom responders declined (76, 77). Moreover, they were reported to be involved in DMSP degradation and also in the production of cobalamin supporting microbial plankton growth (83, 84). Also, A*mylibacter* was previously found attached to particles and bloomed with increased DOM availability (59, 85, 86). *Yoonia-Loktanella* and *Sulfitobacter* were abundant and active with organic matter induction by a phytoplankton bloom in the surface water of the Weddel Sea of the Antarctic Southern Ocean (87).

Rhodobacterales abundance and activity in the summer

HIMB11-, LFER01-, and MED-G52-related genomospecies showed diverse metabolic potentials and activities and were among the most abundant with rapid estimated growth in summer, especially in the Chesapeake Bay. Phosphate concentrations influencing the abundance of HIMB11, LFER01 and MED-G52 suggested that phosphate availability plays a key role in their abundance in these estuaries. The positive correlation of HIMB abundance and silicate concentrations indicated increased diatom presence in the Chesapeake Bay in summer to might enhance this genus (82, 88). Estimated growth rates of HIMB11 were correlated with phosphate concentrations and cell density, also indicating their enhanced ability to replicate during algal blooms. This aligns with previous reports identifying HIMB11 as one of the most common and opportunistic Roseobacters, particularly in summer (89–91). We also observed that the HIMB11-related MAG had higher estimated growth rates in the PA than the FL fractions. HIMB11 was also found abundant and proliferating in the PA fraction from Daya Bay in Southern China (92). Here, the HIMB11-related genomospecies showed significantly higher expression of genes for ribosomal proteins and lower expression of genes for various transporter proteins which supported their higher growth rate estimates in the Chesapeake than the Delaware Bay. In nutritionally or energy-favorable conditions, these genomospecies likely maintained high ribosome and translational machinery concentrations for rapid growth and avoided associated physiological constraints on gene expression by reducing excess levels of certain proteins (like transporters) (93). In addition, nitrogen regulation proteins and ammonium transporters were expressed more in the Chesapeake than the Delaware Bay, indicating the need for N compounds during rapid growth.

LFER01 and MED-G52 genera are less characterized compared to HIMB11 and have only recently been reported (94, 95). MED-G52 could not be analyzed much due to insufficient abundances but we found positive correlations between estimated LFER01 growth rates and light availability in summer when there is high irradiance. In addition, the representative LFER01 genomospecies was abundant in the metatranscriptomes and

had highly expressed genes like *coxL* for energy conservation, and *proX* and *livK* for amino acid transport in summer in the Delaware Bay compared to the Chesapeake Bay but had lower expression of ribosomal proteins which reflected their reduced estimated growth rates. Unlike our study, LFER01 species were seen to significantly affect the oxidation of CO to CO_2 in spring in the Blanes Bay Microbial Observatory near the NW Mediterranean coast (96). LFER01 also showed high cell-specific respiration rates among other genera analyzed in the coastal Gulf of Maine (97). Unlike HIMB11- and LFER01-related genomospecies, changes in gene expression patterns between conditions for ribosomal or other proteins were not observed in MED-G52. However, MED-G52 highly expressed *fdh*/*fdo* genes for formate dehydrogenase are involved in C1 metabolism and may be important for their high abundance and growth rates in summer as previously reported (98).

Conclusion

We identified both *Rhodobacterales* specialists and generalists in the two Mid-Atlantic estuaries, and their presence, activity, and estimated growth rates depended on environmental factors, especially temperature and nutrient availability. Our analysis encompassed well-studied members like *Planktomarina* and HIMB11, as well as lesser-discussed genera like *Boseongicola*, CPC320, and LFER01. Our findings revealed that estimates of growth rate correlated to transcript abundance differences, especially between two MAGs present in the summer, HIMB11 and LFER01, and that there were different controls like phosphate concentrations, evidence of diatom influence (through silicate concentrations), light, and cell density on abundances and estimated growth rates between these MAGs in the two estuaries. This diversity in niche adaptation underscores the importance of *Rhodobacterales* in biogeochemical cycling within estuarine and marine ecosystems. This knowledge and approach used will serve as a foundation for future in-depth analyses of specific taxonomic groups, and their contributions in dynamic estuarine environments.

MATERIALS AND METHODS

Sampling

Surface (~1.5 mbsf) water samples were collected during five cruises on the R/V Sharp using a rosette sampler with associated conductivity, temperature, and depth (CTD) profiles in 2014 and 2015 from the Delaware (DE) and Chesapeake Bays (CP), respectively. The samples were collected from these bays both seasonally and along a salinity gradient to vary environmental conditions to maximize differences between samples. This allowed us to determine major differences in taxonomic, functional potential, and activity/growth rates between different environmental conditions. A map showing the sampling sites was created using ArcGIS software by Esri (Fig. S1) (https://clemson.maps.arcgis.com/home/index.html) (99) . The water quality data were measured using a Sea-Bird data sonde, light intensity and attenuation were measured, and water samples were collected for nutrient concentrations and bacterial production measurements as previously reported (30, 100). Cell separation as large- and small-cell-size fractions by passing water samples sequentially through 0.8- and 0.22-µm-pore-size filters was described previously. The larger and smaller size fractions generally represented the PA and FL assemblages (29, 30). There were 12 metagenomes and 24 duplicating metatranscriptomes from points of the Chesapeake Bay. On the other hand, 24 metagenomes and 35 metatranscriptomes came from the Delaware Bay. Sample labels direct to the collection point and conditions as stated above. TruSeq library preparation kit (Illumina) was used for all metagenomes and metatranscriptomes to get sequences done by the Joint Genome Institute. Collections, extraction, and sequencing of metagenomic and duplicate metatranscriptomic samples as well as MAG generation were previously described (29, 30). Briefly, metagenomes were assembled using

metaSPAdes and MAGs were binned using metaBAT2 (101, 102). Individual metagenomes were used for medium- and high-salinity samples. Pooled metagenomes were also tried for low-salinity samples where *Rhodobacterales* were generally absent.

Quality assessment and taxonomic affiliation of *Rhodobacterales* MAGs

Quast v5.0.2 was used to find MAG characteristics like size, contig numbers, GC content, and N50 value (Data Set S1) (103). CheckM v1.1.3 (lineage_wf default parameters) revealed MAGs with >80% completeness and <5% contamination out of 46 *Rhodobacterales* MAGs from this study (104). Similarly, MAGs with >90% completeness and <10% contamination were added to the data set from a total of 1,753 MAGs found on the NCBI BioSample database when searched with keywords "Rhodobacterales" AND "metagenome" AND "marine" in March 2022. All genomes/MAGs were analyzed using GTDB-Tk v2.1.1 (classify_wf default parameters) to confirm their phylogeny (105). Dereplicated representative *Rhodobacterales* MAGs were obtained using dREP (v3.4.0) based on 95% ANI (106). Amino acid sequences of 28 single-copy ribosomal genes found in >80% of MAGs and genomes were concatenated and aligned using anvi'o v7.1; the alignment was trimmed with trimAl v1.4 to select reliable positions (33, 107). A snapshot maximum-likelihood tree was calculated in RAxMLv8.2.12 with LG substitution matrix and 1,000 bootstrap trees were used to establish support values (32). The tree was visualized and annotated in iTOL v5 to detail the phylogenetic position of the MAGs in relation to reported reference genomes (35). The ANI and average amino acid identity (AAI) between MAGs and reference genomes were calculated using the index_wf --fast -haai option of MiGA v0.7.26.2 (108) and heatmaply v1.4.2 in R/RStudio v4.2.2 was used to plot the resulting AAI matrix (48, 109).

In situ relative abundance and growth rates

Each of the 36 metagenomes and 58 metatranscriptomes from the two bays were mapped to 18 dereplicated MAGs using Bowtie2 v2.4.5 with default parameters and converted into sorted bam files with SAMtools v1.15.1 (110, 111). Read mapping results were summarized using featureCounts v2.0.1 (38). The number of genome equivalents per metagenome was estimated using MicrobeCensus and abundance via RPKG values was calculated as previously described, based on the featureCounts table and the total length of all ORFs in each representative MAG (38–40). A bar graph was made using the ggplot2 library of R/RStudio v4.2.2 (48, 112). In addition, singleM was used to see how much of a metagenome the genomes or assembly represent (36). "corrplot" and "Hmisc" through R were used to generate a plot, showing the effects of environmental factors on average *Rhodobacterales* abundance and estimated growth rates (48, 113–115).

As a proxy to understand the replication of representative *Rhodobacterales* MAGs in sampling sites, PTR, the ratio of sequence coverage near the origin and that near the terminus of replication were obtained using the program Compute PTR (CoPTR) (47, 116) and the heatmaply package in R/RStudio was used to prepare a heatmap from the resulting data (48, 109). The normality of the CoPTR data set was checked using the Shapiro test (117). To see the effects of size fraction and environmental parameters such as season and salinity on CoPTR values of each MAG, a non-parametric Wilcoxon rank test in R was used to determine significantly different CoPTR values between genomospecies in different environments (118). A pairwise Wilcoxon test comparison was done on categories with more than two variables (e.g., seasons—spring, summer, and fall). Spearman correlations of *in situ* growth rates or abundances with environmental parameters were calculated in RStudio using linkET of the vegan package. To measure the maximal growth rates of representative genomospecies, the gRodon package in R was used to calculate codon usage bias (119). This package required Prokka v1.13 to generate gff and ffn files for each representative MAG and calculated maximal growth rates from the codon usage bias for highly expressed genes (119, 120).

Pangenome analyses

To compare the functional potential of *Rhodobacterales* from this estuarine study with known genomes, 46 *Rhodobacterales* MAGs from this study and 57 closely related reference genomes were analyzed with DRAM (42). Also, these MAGs and genomes identified in the phylogenomic tree described above were placed into 11 pangenome groups in anvi'o v7.1 (33). The groups were named based on the genera of MAGs and genomes defined by GTDB-Tk (31, 33). Contig databases generated using anvi'o v7.1 from members of these groups were annotated internally using a gene clustering approach with HMM hits from Clusters of Orthologous Groups (COG), Kyoto Encyclopedia of Genes and Genomes (KEGG), KOfam (a customized KEGG Orthologs (KOs) database), Protein families (Pfam) databases, and externally with Prokka v1.13 (33, 120–123). A summary table was generated from anvi'o containing all gene clusters and associated annotations (33). A percentage of MAGs/genomes within a defined genera harboring a gene of interest was calculated. The matrices of gene abundance percentages in each MAG or genome as a percentage of genera were visualized as heatmaps/bubble plots in RStudio using ggplot2 packages (48, 109, 112). MAGs/genomes were designated as "estuarine," or "marine" based on the reports about where they were found. This information was added to the pangenome as "layers" using the "anvi-import-misc-data" program in anvi'o v7.1. To see the enrichment of COG functions in either marine or estuarine MAGs/genomes, the program "anvi-compute-functional-enrichment-in-pan" in anvi'o v7.1 was used (33). Significantly enriched functions in one group (adjusted q-value < 0.05) were visualized using the ggplot2 package of RStudio (48, 112, 124). Carbohydrate-active enzymes (CAZymes) from representative MAGs were annotated using run_dbcan v4 (44–46). This program found CAZymes in MAGs by comparing their ORFs to the dbcan_seq database which provided CAZyme sequences and annotations (44). CAZymes were categorized into CAZyme families and their abundances in each of the representative MAGs were visualized in RStudio with ggplot2 (48, 112). Moreover, the dbcan-derived diamond output was manually matched with the Prodigal output to get common gene caller IDs (44–46, 125). These IDs were further used to compare gene expressions in different conditions using DESeq2 (50).

Gene expression

Metatranscriptome reads were mapped against representative MAGs with Bowtie2 v2.4.5 as described above (110). Count tables from featureCounts of subread package v.2.0.1 were condensed based on gene clusters identified in anvi'o v7.1 per metatranscriptome (33, 38). Metatranscriptomes were used for analysis in DESeq2 if they had at least ~10,000 reads mapped to genes within a representative MAG (50). From these count tables, principal component analysis (PCA) plots were generated to see how the sample clustered regarding gene expression. For each representative MAG, differentially expressed genes were identified using subsets of feature count tables created based on temporal or spatial differences of samples. The 50 most highly expressed genes from four MAGs, that is, HI_DESum22DL08_bin_21, LF_DESum29NL08_bin_29, ME_DESum29NL08_bin_12, and PI_DESpr20G08_bin_28 (where the first two letters indicated their respective genus names) belonging to HIMB11, LFER01, MED-G52, and *Planktomarina*, respectively, were tabulated and used for visualization. In the figures, manually edited short names/symbols of the genes from the pangenome summary were used. To determine differentially expressed genes, adjusted *P*-values were used from DESeq2 analyses (50). Visualization was done through heatmaps using DESeq2 and pheatmap packages in R (48, 50, 120).

ACKNOWLEDGMENTS

This work was supported by grants from the National Science Foundation (OCE-1261359 and EF-2025541) and the DOE (CSP-1621) to B.J.C. Clemson University is acknowledged for its generous allotment of compute time on the Palmetto Cluster supported by

the National Science Foundation under Grant Nos. MRI# 2024205, MRI# 1725573, and CRI# 2010270. Moreover, the 'omics analyses were made possible, in part, with software support from the Clemson University Genomics and Bioinformatics Facility, which receives support from two Institutional Development Awards (IDeA) from the National Institute of General Medical Sciences of the National Institutes of Health under grant numbers P20GM146584 and P20GM139769.

We thank Dr. Matt Cottrell, Dr. Shen Jean Lim, and Liying Yu for help with sampling and nutrient analyses, Dr. Maximiliano Ortiz for MAG binning, Dr. Jojy John for reviewing and bioinformatic analysis suggestions, and the crew of the R/V Hugh R. Sharp for help with sample collection. We also thank Tijana Galvina del Rio at the Joint Genome Institute for project help.

B.J.C. obtained funding for the study. B.J.C. supervised the project and directed sampling efforts. M.A.A. analyzed the data and wrote the paper with input from B.J.C.

AUTHOR AFFILIATION

[1]Department of Biological Sciences, Clemson University, Clemson, South Carolina, USA

AUTHOR ORCIDs

Mir Alvee Ahmed http://orcid.org/0009-0008-8163-7156
Barbara J. Campbell http://orcid.org/0000-0002-3329-6413

FUNDING

Funder	Grant(s)	Author(s)
National Science Foundation (NSF)	OCE-1261359	Barbara J. Campbell
National Science Foundation (NSF)	EF-2025541	Barbara J. Campbell
Department of Energy | JGI	CSP-1621	Barbara J. Campbell

AUTHOR CONTRIBUTIONS

Mir Alvee Ahmed, Formal analysis, Investigation, Methodology, Software, Visualization, Writing – original draft | Barbara J. Campbell, Conceptualization, Data curation, Funding acquisition, Investigation, Methodology, Project administration, Resources, Software, Supervision, Validation, Writing – review and editing

DATA AVAILABILITY

The metagenomes, metatranscriptomes, and MAGs for this study are available on NCBI under the umbrella project PRJNA432171.

ADDITIONAL FILES

The following material is available online.

Supplemental Material

Data Set S1 (AEM02357-24-s0001.xlsx). Rhodobacterales MAG information with their PTR.
Data Set S2 (AEM02357-24-s0002.xlsx). Gene annotation of Rhodobacterales.
Data Set S3 (AEM02357-24-s0003.xlsx). Rhodobacterales gene expression.
Fig. S1 (AEM02357-24-s0004.tiff). Sampling points.
Fig. S2 (AEM02357-24-s0005.tiff). Representation of Rhodobacterales in samples.
Fig. S3 (AEM02357-24-s0006.tiff). Rhodobacterales relative abundance and environmental factors.
Fig. S4 (AEM02357-24-s0007.tiff). Transporter genes in Rhodobacterales.
Fig. S5 (AEM02357-24-s0008.tiff). CAZymes in Rhodobacterales.

Fig. S6 (AEM02357-24-s0009.tiff). Highly expressed genes of Planktomarina and HIMB11 genomospecies.
Supplemental material (AEM02357-24-s0010.docx). Table S1 and legends for Fig. S1 to S6.

REFERENCES

1. Luo H, Moran MA. 2014. Evolutionary ecology of the marine *Roseobacter* clade. Microbiol Mol Biol Rev 78:573–587. https://doi.org/10.1128/MMBR.00020-14
2. Wagner-Döbler I, Biebl H. 2006. Environmental biology of the marine *Roseobacter* lineage. Annu Rev Microbiol 60:255–280. https://doi.org/10.1146/annurev.micro.60.080805.142115
3. Petersen J, Frank O, Göker M, Pradella S. 2013. Extrachromosomal, extraordinary and essential—the plasmids of the *Roseobacter* clade. Appl Microbiol Biotechnol 97:2805–2815. https://doi.org/10.1007/s00253-013-4746-8
4. Kasalický V, Zeng Y, Piwosz K, Šimek K, Kratochvilová H, Koblížek M. 2018. Aerobic anoxygenic photosynthesis is commonly present within the genus *Limnohabitans*. Appl Environ Microbiol 84:e02116-17. https://doi.org/10.1128/AEM.02116-17
5. Villena-Alemany C, Mujakić I, Porcal P, Koblížek M, Piwosz K. 2023. Diversity dynamics of aerobic anoxygenic phototrophic bacteria in a freshwater lake. Environ Microbiol Rep 15:60–71. https://doi.org/10.1111/1758-2229.13131
6. Buchan A, González JM, Moran MA. 2005. Overview of the marine *Roseobacter* lineage. Appl Environ Microbiol 71:5665–5677. https://doi.org/10.1128/AEM.71.10.5665-5677.2005
7. Voget S, Wemheuer B, Brinkhoff T, Vollmers J, Dietrich S, Giebel H-A, Beardsley C, Sardemann C, Bakenhus I, Billerbeck S, Daniel R, Simon M. 2015. Adaptation of an abundant *Roseobacter* RCA organism to pelagic systems revealed by genomic and transcriptomic analyses. ISME J 9:371–384. https://doi.org/10.1038/ismej.2014.134
8. Buchan A, González JM, Chua MJ. 2019. Aerobic hydrocarbon-degrading *Alphaproteobacteria*: *Rhodobacteraceae* (*Roseobacter*). Taxon Genomics Ecophysiol Hydrocarb Microbes:93–104. https://doi.org/10.1007/978-3-030-14796-9_8
9. O'Brien J, McParland EL, Bramucci AR, Siboni N, Ostrowski M, Kahlke T, Levine NM, Brown MV, van de Kamp J, Bodrossy L, Messer LF, Petrou K, Seymour JR. 2022. Biogeographical and seasonal dynamics of the marine *Roseobacter* community and ecological links to DMSP-producing phytoplankton. ISME Commun 2:16. https://doi.org/10.1038/s43705-022-00099-3
10. Moran MA, Belas R, Schell MA, González JM, Sun F, Sun S, Binder BJ, Edmonds J, Ye W, Orcutt B, Howard EC, Meile C, Palefsky W, Goesmann A, Ren Q, Paulsen I, Ulrich LE, Thompson LS, Saunders E, Buchan A. 2007. Ecological genomics of marine *Roseobacters*. Appl Environ Microbiol 73:4559–4569. https://doi.org/10.1128/AEM.02580-06
11. Moran MA, Buchan A, González JM, Heidelberg JF, Whitman WB, Kiene RP, Henriksen JR, King GM, Belas R, Fuqua C, et al. 2004. Genome sequence of *Silicibacter pomeroyi* reveals adaptations to the marine environment. Nature 432:910–913. https://doi.org/10.1038/nature03170
12. Arora-Williams K, Holder C, Secor M, Ellis H, Xia M, Gnanadesikan A, Preheim SP. 2022. Abundant and persistent sulfur-oxidizing microbial populations are responsive to hypoxia in the Chesapeake Bay. Environ Microbiol 24:2315–2332. https://doi.org/10.1111/1462-2920.15976
13. Newton RJ, Griffin LE, Bowles KM, Meile C, Gifford S, Givens CE, Howard EC, King E, Oakley CA, Reisch CR, Rinta-Kanto JM, Sharma S, Sun S, Varaljay V, Vila-Costa M, Westrich JR, Moran MA. 2010. Genome characteristics of a generalist marine bacterial lineage. ISME J 4:784–798. https://doi.org/10.1038/ismej.2009.150
14. Kan J, Hanson TE, Ginter JM, Wang K, Chen F. 2005. Metaproteomic analysis of Chesapeake Bay microbial communities. Saline Syst 1:7. https://doi.org/10.1186/1746-1448-1-7
15. Jonas RB. 1997. Trophic models. Comp Gen Pharmacol 620:612–620. https://doi.org/10.1093/icb/37.6.612
16. Griffith P, Shiah F F-K, Gloersen K, Ducklow H, Fletcher M. 1994. Activity and distribution of attached bacteria in Chesapeake Bay. Mar Ecol Prog Ser 108:1–10. https://doi.org/10.3354/meps108001
17. Gay P, O'Donnell J. 2009. Comparison of the salinity structure of the Chesapeake Bay, the Delaware Bay and Long Island Sound using a linearly tapered advection-dispersion model. Estuaries Coast 32:68–87. https://doi.org/10.1007/s12237-008-9101-4
18. Tian R, Cerco CF, Bhatt G, Linker LC, Shenk GW. 2022. Mechanisms controlling climate warming impact on the occurrence of hypoxia in Chesapeake Bay. J Am Water Resour Assoc 58:855–875. https://doi.org/10.1111/1752-1688.12907
19. Kan J, Suzuki MT, Wang K, Evans SE, Chen F. 2007. High temporal but low spatial heterogeneity of bacterioplankton in the Chesapeake Bay. Appl Environ Microbiol 73:6776–6789. https://doi.org/10.1128/AEM.00541-07
20. Malone TC, Crocker LH, Pike SE, Wendler BW. 1988. Influences of river flow on the dynamics of phytoplankton production in a partially stratified estuary. Mar Ecol Prog Ser 48:235–249. https://doi.org/10.3354/meps048235
21. Sharp JH, Cifuentes LA, Coffin RB, Pennock JR, Wong K-C. 1986. The influence of river variability on the circulation, chemistry, and microbiology of the Delaware Estuary. Estuaries 9:261. https://doi.org/10.2307/1352098
22. Aristizábal M, Chant R, Aristizábal M. 2014. Mechanisms driving stratification in Delaware Bay estuary. Ocean Dyn 64:1615–1629. https://doi.org/10.1007/s10236-014-0770-1
23. Harding LW, Meeson BW, Fisher TR. 1986. Phytoplankton production in two east coast estuaries: photosynthesis-light functions and patterns of carbon assimilation in Chesapeake and Delaware Bays. Estuar Coast Shelf Sci 23:773–806. https://doi.org/10.1016/0272-7714(86)90074-0
24. Sharp JH, Yoshiyama K, Parker AE, Schwartz MC, Curless SE, Beauregard AY, Ossolinski JE, Davis AR. 2009. A biogeochemical view of estuarine eutrophication: seasonal and spatial trends and correlations in the Delaware Estuary. Estuaries Coast 32:1023–1043. https://doi.org/10.1007/s12237-009-9210-8
25. Murphy RR, Kemp WM, Ball WP. 2011. Long-term trends in Chesapeake Bay seasonal hypoxia, stratification, and nutrient loading. Estuaries Coast 34:1293–1309. https://doi.org/10.1007/s12237-011-9413-7
26. Kan J, Crump BC, Wang K, Chen F. 2006. Bacterioplankton community in Chesapeake Bay: predictable or random assemblages. Limnol Oceanogr 51:2157–2169. https://doi.org/10.4319/lo.2006.51.5.2157
27. Campbell BJ, Kirchman DL. 2013. Bacterial diversity, community structure and potential growth rates along an estuarine salinity gradient. ISME J 7:210–220. https://doi.org/10.1038/ismej.2012.93
28. Wang H, Zhang C, Chen F, Kan J. 2020. Spatial and temporal variations of bacterioplankton in the Chesapeake Bay: a re-examination with high-throughput sequencing analysis. Limnol Ocean 65:3032–3045. https://doi.org/10.1002/lno.11572
29. Ahmed MA, Lim SJ, Campbell BJ. 2021. Metagenomes, metatranscriptomes, and metagenome-assembled genomes from Chesapeake and Delaware Bay (USA) water samples. Microbiol Resour Announc 10:e0026221. https://doi.org/10.1128/MRA.00262-21
30. Maresca JA, Miller KJ, Keffer JL, Sabanayagam CR, Campbell BJ. 2018. Distribution and diversity of rhodopsin-producing microbes in the Chesapeake Bay. Appl Environ Microbiol 84:e00137-18. https://doi.org/10.1128/AEM.00137-18
31. Chaumeil PA, Mussig AJ, Hugenholtz P, Parks DH. 2019. GTDB-Tk: a toolkit to classify genomes with the genome taxonomy database. Bioinformatics 36:1925–1927. https://doi.org/10.1093/bioinformatics/btz848
32. Stamatakis A. 2014. RAxML version 8: a tool for phylogenetic analysis and post-analysis of large phylogenies. Bioinformatics 30:1312–1313. https://doi.org/10.1093/bioinformatics/btu033
33. Eren AM, Esen ÖC, Quince C, Vineis JH, Morrison HG, Sogin ML, Delmont TO. 2015. Anvi'o: an advanced analysis and visualization platform for 'omics data. PeerJ 3:e1319. https://doi.org/10.7717/peerj.1319
34. Guindon S, Gascuel O. 2003. A simple, fast, and accurate algorithm to estimate large phylogenies by maximum likelihood. Syst Biol 52:696–704. https://doi.org/10.1080/10635150390235520

35. Letunic I, Bork P. 2021. Interactive Tree Of Life (iTOL) v5: an online tool for phylogenetic tree display and annotation. Nucleic Acids Res 49:W293–W296. https://doi.org/10.1093/nar/gkab301
36. Woodcroft BJ, Aroney STN, Zhao R, Cunningham M, Mitchell JAM, Blackall L, Tyson GW. 2024. SingleM and Sandpiper: robust microbial taxonomic profiles from metagenomic data. bioRxiv. https://doi.org/10.1101/2024.01.30.578060
37. Menzel P, Ng KL, Krogh A. 2016. Fast and sensitive taxonomic classification for metagenomics with Kaiju. Nat Commun 7:11257. https://doi.org/10.1038/ncomms11257
38. Liao Y, Smyth GK, Shi W. 2014. featureCounts: an efficient general purpose program for assigning sequence reads to genomic features. Bioinformatics 30:923–930. https://doi.org/10.1093/bioinformatics/btt656
39. Reji L, Francis CA. 2020. Metagenome-assembled genomes reveal unique metabolic adaptations of a basal marine Thaumarchaeota lineage. ISME J 14:2105–2115. https://doi.org/10.1038/s41396-020-0675-6
40. Nayfach S, Pollard KS. 2015. Average genome size estimation improves comparative metagenomics and sheds light on the functional ecology of the human microbiome. Genome Biol 16:51. https://doi.org/10.1186/s13059-015-0611-7
41. Myers L, Sirois MJ. 2004. Spearman correlation coefficients, differences between. Encycl Stat Sci 12. https://doi.org/10.1002/0471667196
42. Shaffer M, Borton MA, McGivern BB, Zayed AA, La Rosa SL, Solden LM, Liu P, Narrowe AB, Rodríguez-Ramos J, Bolduc B, Gazitúa MC, Daly RA, Smith GJ, Vik DR, Pope PB, Sullivan MB, Roux S, Wrighton KC. 2020. DRAM for distilling microbial metabolism to automate the curation of microbiome function. Nucleic Acids Res 48:8883–8900. https://doi.org/10.1093/nar/gkaa621
43. Garron M-L, Henrissat B. 2019. The continuing expansion of CAZymes and their families. Curr Opin Chem Biol 53:82–87. https://doi.org/10.1016/j.cbpa.2019.08.004
44. Huang L, Zhang H, Wu P, Entwistle S, Li X, Yohe T, Yi H, Yang Z, Yin Y. 2018. dbCAN-seq: a database of carbohydrate-active enzyme (CAZyme) sequence and annotation. Nucleic Acids Res 46:D516–D521. https://doi.org/10.1093/nar/gkx894
45. Zhang H, Yohe T, Huang L, Entwistle S, Wu P, Yang Z, Busk PK, Xu Y, Yin Y. 2018. dbCAN2: a meta server for automated carbohydrate-active enzyme annotation. Nucleic Acids Res 46:W95–W101. https://doi.org/10.1093/nar/gky418
46. Zheng J, Ge Q, Yan Y, Zhang X, Huang L, Yin Y. 2023. dbCAN3: automated carbohydrate-active enzyme and substrate annotation. Nucleic Acids Res 51:W115–W121. https://doi.org/10.1093/nar/gkad328
47. Joseph TA, Chlenski P, Litman A, Korem T, Pe'er I. 2022. Accurate and robust inference of microbial growth dynamics from metagenomic sequencing reveals personalized growth rates. Genome Res 32:558–568. https://doi.org/10.1101/gr.275533.121
48. R Core Team. 2022. R: a language and environment for statistical computing. Vienna, Austria.
49. Long AM, Hou S, Ignacio-Espinoza JC, Fuhrman JA. 2021. Benchmarking microbial growth rate predictions from metagenomes. ISME J 15:183–195. https://doi.org/10.1038/s41396-020-00773-1
50. Love MI, Huber W, Anders S. 2014. Moderated estimation of fold change and dispersion for RNA-seq data with DESeq2. Genome Biol 15:550. https://doi.org/10.1186/s13059-014-0550-8
51. Giebel HA, Kalhoefer D, Lemke A, Thole S, Gahl-Janssen R, Simon M, Brinkhoff T. 2011. Distribution of *Roseobacter* RCA and SAR11 lineages in the North Sea and characteristics of an abundant RCA isolate. ISME J 5:8–19. https://doi.org/10.1038/ismej.2010.87
52. Garrity GM, Bell JA, Lilburn T. 2015. *Rhodobacteraceae fam. nov*, p 1–2. In Bergey's manual of systematics of archaea and bacteria
53. Polz MF, Hunt DE, Preheim SP, Weinreich DM. 2006. Patterns and mechanisms of genetic and phenotypic differentiation in marine microbes. Philos Trans R Soc Lond B Biol Sci 361:2009–2021. https://doi.org/10.1098/rstb.2006.1928
54. Tada Y, Taniguchi A, Nagao I, Miki T, Uematsu M, Tsuda A, Hamasaki K. 2011. Differing growth responses of major phylogenetic groups of marine bacteria to natural phytoplankton blooms in the western North Pacific Ocean. Appl Environ Microbiol 77:4055–4065. https://doi.org/10.1128/AEM.02952-10
55. Giebel HA, Wolterink M, Brinkhoff T, Simon M. 2019. Complementary energy acquisition via aerobic anoxygenic photosynthesis and carbon monoxide oxidation by *Planktomarina temperata* of the *Roseobacter* group. FEMS Microbiol Ecol 95:fiz050. https://doi.org/10.1093/femsec/fiz050
56. Isaac A, Francis B, Amann RI, Amin SA. 2021. Tight adherence (Tad) pilus genes indicate putative niche differentiation in phytoplankton bloom associated *Rhodobacterales*. Front Microbiol 12:718297. https://doi.org/10.3389/fmicb.2021.718297
57. Sieradzki ET, Morando M, Fuhrman JA. 2021. Metagenomics and quantitative stable isotope probing offer insights into metabolism of polycyclic aromatic hydrocarbon degraders in chronically polluted seawater. mSystems 6:e00245-21. https://doi.org/10.1128/mSystems.00245-21
58. Moran MA, Miller WL. 2007. Resourceful heterotrophs make the most of light in the coastal ocean. Nat Rev Microbiol 5:792–800. https://doi.org/10.1038/nrmicro1746
59. Taylor JD, Cunliffe M. 2017. Coastal bacterioplankton community response to diatom-derived polysaccharide microgels. Environ Microbiol Rep 9:151–157. https://doi.org/10.1111/1758-2229.12513
60. Cooper MB, Kazamia E, Helliwell KE, Kudahl UJ, Sayer A, Wheeler GL, Smith AG. 2019. Cross-exchange of B-vitamins underpins a mutualistic interaction between *Ostreococcus tauri* and *Dinoroseobacter shibae*. ISME J 13:334–345. https://doi.org/10.1038/s41396-018-0274-y
61. Moran MA, González JM, Kiene RP. 2003. Linking a bacterial taxon to sulfur cycling in the sea: studies of the marine *Roseobacter* group. Geomicrobiol J 20:375–388. https://doi.org/10.1080/01490450303901
62. Hernández L, Vicens A, Eguiarte LE, Souza V, De Anda V, González JM. 2020. Evolutionary history of dimethylsulfoniopropionate (DMSP) demethylation enzyme DmdA in marine bacteria. PeerJ 8:e9861. https://doi.org/10.7717/peerj.9861
63. Preheim S, Morris S, Zhang Y, Holder C, Arora-Williams K, Gensbigler P, Hinton A, Jin R, Pradal M-A, Gnanadesikan A. 2023. Major trends and environmental correlates of spatiotemporal shifts in the distribution of genes compared to a biogeochemical model simulation in the Chesapeake Bay. bioRxiv. https://doi.org/10.1101/2023.01.09.523340
64. Waidner LA, Kirchman DL. 2008. Diversity and distribution of ecotypes of the aerobic anoxygenic phototrophy gene *pufM* in the Delaware estuary. Appl Environ Microbiol 74:4012–4021. https://doi.org/10.1128/AEM.02324-07
65. Alonso-Sáez L, Morán XAG, González JM. 2020. Transcriptional patterns of biogeochemically relevant marker genes by temperate marine bacteria. Front Microbiol 11:465. https://doi.org/10.3389/fmicb.2020.00465
66. Fecskeová LK, Piwosz K, Hanusová M, Nedoma J, Znachor P, Koblížek M. 2019. Diel changes and diversity of *pufM* expression in freshwater communities of anoxygenic phototrophic bacteria. Sci Rep 9:18766. https://doi.org/10.1038/s41598-019-55210-x
67. Tada Y, Makabe R, Kasamatsu-Takazawa N, Taniguchi A, Hamasaki K. 2013. Growth and distribution patterns of *Roseobacter*/*Rhodobacter*, SAR11, and *Bacteroidetes* lineages in the Southern Ocean. Polar Biol 36:691–704. https://doi.org/10.1007/s00300-013-1294-8
68. Campbell BJ, Yu L, Heidelberg JF, Kirchman DL. 2011. Activity of abundant and rare bacteria in a coastal ocean. Proc Natl Acad Sci USA 108:12776–12781. https://doi.org/10.1073/pnas.1101405108
69. Hewitt OH, Shaikh HM. 2021. The rhythm of many: biological rhythms in the marine environment, from macro-scale planktonic ecosystems to micro-scale holobionts. Front Mar Sci 8. https://doi.org/10.3389/fmars.2021.744169
70. Lankiewicz TS, Cottrell MT, Kirchman DL. 2016. Growth rates and rRNA content of four marine bacteria in pure cultures and in the Delaware estuary. ISME J 10:823–832. https://doi.org/10.1038/ismej.2015.156
71. Bouchachi N, Obernosterer I, Carpaneto Bastos C, Li F, Scenna L, Marie B, Crispi O, Catala P, Ortega-Retuerta E. 2023. Effects of phosphorus limitation on the bioavailability of DOM released by marine heterotrophic prokaryotes. Microb Ecol 86:1961–1971. https://doi.org/10.1007/s00248-023-02201-1
72. Luo H, Benner R, Long RA, Hu J. 2009. Subcellular localization of marine bacterial alkaline phosphatases. Proc Natl Acad Sci USA 106:21219–21223. https://doi.org/10.1073/pnas.0907586106
73. Allen JT, Brown L, Sanders R, Moore CM, Mustard A, Fielding S, Lucas M, Rixen M, Savidge G, Henson S, Mayor D. 2005. Diatom carbon export enhanced by silicate upwelling in the northeast Atlantic. Nature 437:728–732. https://doi.org/10.1038/nature03948

74. Ferrer-González FX, Widner B, Holderman NR, Glushka J, Edison AS, Kujawinski EB, Moran MA. 2021. Resource partitioning of phytoplankton metabolites that support bacterial heterotrophy. ISME J 15:762–773. https://doi.org/10.1038/s41396-020-00811-y
75. Ding W, Wang S, Qin P, Fan S, Su X, Cai P, Lu J, Cui H, Wang M, Shu Y, Wang Y, Fu HH, Zhang YZ, Li YX, Zhang W. 2023. Anaerobic thiosulfate oxidation by the *Roseobacter* group is prevalent in marine biofilms. Nat Commun 14:2033. https://doi.org/10.1038/s41467-023-37759-4
76. Liu Y, Blain S, Crispi O, Rembauville M, Obernosterer I. 2020. Seasonal dynamics of prokaryotes and their associations with diatoms in the Southern Ocean as revealed by an autonomous sampler. Environ Microbiol 22:3968–3984. https://doi.org/10.1111/1462-2920.15184
77. Wang F-Q, Bartosik D, Sidhu C, Siebers R, Lu D-C, Trautwein-Schult A, Becher D, Huettel B, Rick J, Kirstein IV, Wiltshire KH, Schweder T, Fuchs BM, Bengtsson MM, Teeling H, Amann RI. 2024. Particle-attached bacteria act as gatekeepers in the decomposition of complex phytoplankton polysaccharides. Microbiome 12:32. https://doi.org/10.1186/s40168-024-01757-5
78. Zhang H, Tan Y, Zhou Y, Liu J, Xia X. 2024. Light-dark fluctuated metabolic features of diazotrophic and non-diazotrophic cyanobacteria and their coexisting bacteria. Sci Total Environ 910:168702. https://doi.org/10.1016/j.scitotenv.2023.168702
79. Bunse C, Koch H, Breider S, Simon M, Wietz M. 2021. Sweet spheres: succession and CAZyme expression of marine bacterial communities colonizing a mix of alginate and pectin particles. Environ Microbiol 23:3130–3148. https://doi.org/10.1111/1462-2920.15536
80. Wang CN, Liu Y, Wang J, Du ZJ, Wang MY. 2021. *Sulfitobacter algicola* sp. nov., isolated from green algae. Arch Microbiol 203:2351–2356. https://doi.org/10.1007/s00203-021-02213-w
81. Tang K, Yang Y, Lin D, Li S, Zhou W, Han Y, Liu K, Jiao N. 2016. Genomic, physiologic, and proteomic insights into metabolic versatility in *Roseobacter* clade bacteria isolated from deep-sea water. Sci Rep 6:35528. https://doi.org/10.1038/srep35528
82. Pennock JR, Sharp JH. 1986. Phytoplankton production in the Delaware Estuary: temporal and spatial variability. Mar Ecol Prog Ser 34:143–155. https://doi.org/10.3354/meps034143
83. Joglar V, Álvarez-Salgado XA, Gago-Martinez A, Leao JM, Pérez-Martínez C, Pontiller B, Lundin D, Pinhassi J, Fernández E, Teira E. 2021. Cobalamin and microbial plankton dynamics along a coastal to offshore transect in the Eastern North Atlantic Ocean. Environ Microbiol 23:1559–1583. https://doi.org/10.1111/1462-2920.15367
84. Wang S, Zhang N, Teng Z, Wang X, Todd JD, Zhang Y, Cao H, Li C. 2023. A new dimethylsulfoniopropionate lyase of the cupin superfamily in marine bacteria. Environ Microbiol 25:1238–1249. https://doi.org/10.1111/1462-2920.16355
85. Wietz M, Bienhold C, Metfies K, Torres-Valdés S, von Appen W-J, Salter I, Boetius A. 2021. The polar night shift: seasonal dynamics and drivers of Arctic Ocean microbiomes revealed by autonomous sampling. ISME Commun 1:76. https://doi.org/10.1038/s43705-021-00074-4
86. Costas-Selas C, Martínez-García S, Logares R, Hernández-Ruiz M, Teira E. 2023. Role of bacterial community composition as a driver of the small-sized phytoplankton community structure in a productive coastal system. Microb Ecol 86:777–794. https://doi.org/10.1007/s00248-022-02125-2
87. Piontek J, Meeske C, Hassenrück C, Engel A, Jürgens K. 2022. Organic matter availability drives the spatial variation in the community composition and activity of Antarctic marine bacterioplankton. Environ Microbiol 24:4030–4048. https://doi.org/10.1111/1462-2920.16087
88. Harding, LW, Mallonee ME, Perry ES, Miller WD, Adolf JE, Gallegos CL, Paerl HW. 2016. Variable climatic conditions dominate recent phytoplankton dynamics in Chesapeake Bay. Sci Rep 6:1–16. https://doi.org/10.1038/srep23773
89. Korlević M, Markovski M, Herndl GJ, Najdek M. 2022. Temporal variation in the prokaryotic community of a nearshore marine environment. Sci Rep 12:121 https://doi.org/10.1038/s41598-022-20954-6
90. Beauvais M, Schatt P, Montiel L, Logares R, Galand PE, Bouget FY. 2023. Functional redundancy of seasonal vitamin B_{12} biosynthesis pathways in coastal marine microbial communities. Environ Microbiol 25:3753–3770. https://doi.org/10.1111/1462-2920.16545
91. Chénard C, Wijaya W, Vaulot D, Lopes Dos Santos A, Martin P, Kaur A, Lauro FM. 2019. Temporal and spatial dynamics of bacteria, archaea and protists in equatorial coastal waters. Sci Rep 9:16390. https://doi.org/10.1038/s41598-019-52648-x
92. Shi R, Han T, Qi Z, Huang H. 2024. Responses of attached bacterial communities to blooms of the swimming shelled pteropod *Creseis acicula* in Daya Bay, southern China. FEMS Microbiol Ecol 100:fiae034. https://doi.org/10.1093/femsec/fiae034
93. Scott M, Hwa T. 2023. Shaping bacterial gene expression by physiological and proteome allocation constraints. Nat Rev Microbiol 21:327–342. https://doi.org/10.1038/s41579-022-00818-6
94. IvaS, DanijelaŠ, Cristian , V-A, Željka T, Frano M, Ana VrdoljakT. 2024. Ecology of aerobic anoxygenic phototrophs on a fine-scale taxonomic resolution in Adriatic Sea unravelled by unsupervised neural network. Environ Microbiome. https://doi.org/10.1186/s40793-024-00573-6
95. Prabhu A, Tule S, Chuvochina M, Bodén M, McIlroy SJ, Zaugg J, Rinke C. 2024. Machine learning and metagenomics identifies uncharacterized taxa inferred to drive biogeochemical cycles in a subtropical hypereutrophic estuary. ISME Comm 4:ycae067. https://doi.org/10.1093/ismeco/ycae067
96. Auladell A, Ferrera I, Montiel Fontanet L, Santos Júnior CD, Sebastián M, Logares R, Gasol JM. 2023. Seasonality of biogeochemically relevant microbial genes in a coastal ocean microbiome. Environ Microbiol 25:1465–1483. https://doi.org/10.1111/1462-2920.16367
97. Munson-McGee JH, Lindsay MR, Sintes E, Brown JM, D'Angelo T, Brown J, Lubelczyk LC, Tomko P, Emerson D, Orcutt BN, Poulton NJ, Herndl GJ, Stepanauskas R. 2022. Decoupling of respiration rates and abundance in marine prokaryoplankton. Nature 612:764–770. https://doi.org/10.1038/s41586-022-05505-3
98. Chen Y. 2012. Comparative genomics of methylated amine utilization by marine *Roseobacter* clade bacteria and development of functional gene markers (*tmm*, *gmaS*). Environ Microbiol 14:2308–2322. https://doi.org/10.1111/j.1462-2920.2012.02765.x
99. An introduction to ArcGIS Online. 2022. Environmental Systems Research Institute. https://doc.arcgis.com/en/arcgis-online/get-started/what-is-agol.htm.
100. Preen K, Kirchman D. 2004. Microbial respiration and production in the Delaware Estuary. Aquat Microb Ecol 37:109–119. https://doi.org/10.3354/ame037109
101. Kang DD, Froula J, Egan R, Wang Z. 2015. MetaBAT, an efficient tool for accurately reconstructing single genomes from complex microbial communities. PeerJ 3:e1165. https://doi.org/10.7717/peerj.1165
102. Nurk S, Meleshko D, Korobeynikov A, Pevzner PA. 2017. MetaSPAdes: a new versatile metagenomic assembler. Genome Res 27:824–834. https://doi.org/10.1101/gr.213959.116
103. Gurevich A, Saveliev V, Vyahhi N, Tesler G. 2013. QUAST: quality assessment tool for genome assemblies. Bioinformatics 29:1072–1075. https://doi.org/10.1093/bioinformatics/btt086
104. Parks DH, Imelfort M, Skennerton CT, Hugenholtz P, Tyson GW. 2015. CheckM: assessing the quality of microbial genomes recovered from isolates, single cells, and metagenomes. Genome Res 25:1043–1055. https://doi.org/10.1101/gr.186072.114
105. Parks DH, Chuvochina M, Waite DW, Rinke C, Skarshewski A, Chaumeil PA, Hugenholtz P. 2018. A standardized bacterial taxonomy based on genome phylogeny substantially revises the tree of life. Nat Biotechnol 36:996–1004. https://doi.org/10.1038/nbt.4229
106. Olm MR, Brown CT, Brooks B, Banfield JF. 2017. DRep: a tool for fast and accurate genomic comparisons that enables improved genome recovery from metagenomes through de-replication. ISME J 11:2864–2868. https://doi.org/10.1038/ismej.2017.126
107. Capella-Gutiérrez S, Silla-Martínez JM, Gabaldón T. 2009. trimAl: a tool for automated alignment trimming in large-scale phylogenetic analyses. Bioinformatics 25:1972–1973. https://doi.org/10.1093/bioinformatics/btp348
108. Rodriguez-R LM, Gunturu S, Harvey WT, Rosselló-Mora R, Tiedje JM, Cole JR, Konstantinidis KT. 2018. The Microbial Genomes Atlas (MiGA) webserver: taxonomic and gene diversity analysis of Archaea and Bacteria at the whole genome level. Nucleic Acids Res 46:W282–W288. https://doi.org/10.1093/nar/gky467
109. Galili T, O'Callaghan A, Sidi J, Sievert C. 2018. heatmaply: an R package for creating interactive cluster heatmaps for online publishing. Bioinformatics 34:1600–1602. https://doi.org/10.1093/bioinformatics/btx657
110. Langmead B, Salzberg SL. 2012. Fast gapped-read alignment with Bowtie 2. Nat Methods 9:357–359. https://doi.org/10.1038/nmeth.1923
111. Li H, Handsaker B, Wysoker A, Fennell T, Ruan J, Homer N, Marth G, Abecasis G, Durbin R, 1000 Genome Project Data Processing Subgroup. 2009. The sequence alignment/map format and SAMtools.

Bioinformatics 25:2078–2079. https://doi.org/10.1093/bioinformatics/btp352
112. Wickham MH. 2014. Package "ggplot2" type package title an implementation of the grammar of graphics
113. Capblancq T, Forester BR. 2021. Redundancy analysis: a Swiss Army Knife for landscape genomics. Methods Ecol Evol 12:2298–2309. https://doi.org/10.1111/2041-210X.13722
114. Oksanen J, Simpson GL. 2009. The vegan package
115. Wei T, Simko V, Levy M, Xie Y, Jin Y, Zemla J, Freidank M, Cai J, Protivinsky T. 2017. Package "corrplot" title visualization of a correlation matrix NeedsCompilation no
116. Korem T, Zeevi D, Suez J, Weinberger A, Avnit-Sagi T, Pompan-Lotan M, Matot E, Jona G, Harmelin A, Cohen N, Sirota-Madi A, Thaiss CA, Pevsner-Fischer M, Sorek R, Xavier R, Elinav E, Segal E. 2015. Growth dynamics of gut microbiota in health and disease inferred from single metagenomic samples. Science 349:1101–1106. https://doi.org/10.1126/science.aac4812
117. Royston JP. 1982. An extension of Shapiro and Wilk's W test for normality to large samples. Appl Stat 31:115. https://doi.org/10.2307/2347973
118. Bauer DF. 1972. Constructing confidence sets using rank statistics. J Am Stat Assoc 67:687. https://doi.org/10.2307/2284469
119. Weissman JL, Hou S, Fuhrman JA. 2021. Estimating maximal microbial growth rates from cultures, metagenomes, and single cells via codon usage patterns. Proc Natl Acad Sci U S A 118:e2016810118. https://doi.org/10.1073/pnas.2016810118
120. Seemann T. 2014. Prokka: rapid prokaryotic genome annotation. Bioinformatics 30:2068–2069. https://doi.org/10.1093/bioinformatics/btu153
121. Tatusov RL, Galperin MY, Natale DA, Koonin EV. 2000. The COG database: a tool for genome-scale analysis of protein functions and evolution. Nucleic Acids Res 28:33–36. https://doi.org/10.1093/nar/28.1.33
122. Kanehisa M, Goto S. 2000. KEGG: kyoto encyclopedia of genes and genomes. Nucleic Acids Res 28:27–30. https://doi.org/10.1093/nar/28.1.27
123. Bateman A, Coin L, Durbin R, Finn RD, Hollich V, Griffiths-Jones S, Khanna A, Marshall M, Moxon S, Sonnhammer ELL, Studholme DJ, Yeats C, Eddy SR. 2004. The Pfam protein families database. Nucleic Acids Res 32:D138–D141. https://doi.org/10.1093/nar/gkh121
124. Shaiber A, Willis AD, Delmont TO, Roux S, Chen L-X, Schmid AC, Yousef M, Watson AR, Lolans K, Esen ÖC, Lee STM, Downey N, Morrison HG, Dewhirst FE, Mark Welch JL, Eren AM. 2020. Functional and genetic markers of niche partitioning among enigmatic members of the human oral microbiome. Genome Biol 21:292. https://doi.org/10.1186/s13059-020-02195-w
125. Hyatt D, Chen G-L, Locascio PF, Land ML, Larimer FW, Hauser LJ. 2010. Prodigal: prokaryotic gene recognition and translation initiation site identification. BMC Bioinformatics 11:119. https://doi.org/10.1186/1471-2105-11-119